



The geomorphological record of an ice stream to ice shelf transition in Northeast Greenland

Timothy P. Lane¹  | Christopher Darvill² | Brice R. Rea³ | Michael J. Bentley⁴ | James A. Smith⁵ | Stewart S.R. Jamieson⁴ | Colm Ó Cofaigh⁴ | David H. Roberts⁴ 

¹School of Biological and Environmental Sciences, Liverpool John Moores University, Liverpool, UK

²Department of Geography, The University of Manchester, Manchester, UK

³School of Geosciences, University of Aberdeen, Aberdeen, UK

⁴Department of Geography, Durham University, Durham, UK

⁵British Antarctic Survey, Natural Environment Research Council, Cambridge, UK

Correspondence

Timothy P. Lane, School of Biological and Environmental Sciences, Liverpool John Moores University, Liverpool, UK.

Email: t.p.lane@ljmu.ac.uk

Funding information

Natural Environment Research Council, Grant/Award Number: NE/N011228/1

Abstract

Understanding ice stream dynamics over decadal to millennial timescales is crucial for improving numerical model projections of ice sheet behaviour and future ice loss. In marine-terminating settings, ice shelves play a critical role in controlling ice-stream grounding line stability and ice flux to the ocean, but few studies have investigated the terrestrial lateral geomorphological imprint of ice shelves during deglaciation. Here, we document the terrestrial deglacial landsystem of Nioghalvfjærdsfjorden Glacier (79N) in northeast Greenland, following the Last Glacial Maximum, and the margin's lateral transition to a floating ice shelf. High-elevation areas are influenced by local ice caps and display autochthonous to allochthonous blockfields that mark the interaction of local ice caps with the ice stream below. A thermal transition from cold- to warm-based ice is denoted by the emplacement of erratics onto allochthonous blockfields. Below ~600 m above sea level (a.s.l.) glacially abraded bedrock surfaces and assemblages of lateral moraines, 'hummocky' moraine, fluted terrain, and ice-contact deltas record the former presence of warm-based ice and thinning of the grounded ice stream margin through time. In the outer fjord a range of landforms such as ice shelf moraines, dead-ice topography, and ice marginal glaciofluvial outwash was produced by an ice shelf during deglaciation. Along the mid- and inner-fjord areas this ice shelf signal is absent, suggesting ice shelf disintegration prior to grounding line retreat under tide-water conditions. However, below the marine limit, the geomorphological record along the fjord indicates the expansion of the 79N ice shelf during the Neoglacial, which culminated in the Little Ice Age. This was followed by 20th century recession, with the development of a suite of compressional ice shelf moraines, ice-marginal fluvio-glacial corridors, kame terraces, dead-ice terrain, and crevasse infill ridges. These mark rapid ice shelf thinning and typify the present-day ice shelf landsystem in a warming climate.

KEYWORDS

ice stream, ice shelf, geomorphology, Greenland, palaeoglaciology

1 | INTRODUCTION

Marine terminating ice streams and their ice shelves are critical components of the global climate system, responding to climate forcings

(Goldberg et al., 2009; Gudmundsson, 2013; Reese et al., 2018). Ice shelves buttress ice streams and modulate grounding line dynamics (Scambos et al., 2004). The recent and potential future loss of ice shelves in Greenland and Antarctica could lead to debuttressing of

This is an open access article under the terms of the [Creative Commons Attribution](https://creativecommons.org/licenses/by/4.0/) License, which permits use, distribution and reproduction in any medium, provided the original work is properly cited.

© 2023 The Authors. *Earth Surface Processes and Landforms* published by John Wiley & Sons Ltd.

outlet glaciers and ice velocity increases, resulting in rapid ice flux to the oceans and significant sea-level rise (Goldberg et al., 2009; Gudmundsson, 2013; Reese et al., 2018).

Determining the factors that control ice stream and ice shelf stability is important for understanding ice dynamics and for improving models of future ice sheet evolution. Satellite observations have facilitated estimation of grounding line dynamics and rates of ice shelf disintegration over the last 40 years (Hogg et al., 2016; Xie et al., 2018), and sub-ice shelf sediment records from some parts of Antarctica have constrained oscillations over the last 150 years (Smith et al., 2017, 2019). Combined with modern observations, recent and contemporary rates of ice shelf change and grounding line migration are relatively well known. However, longer-term records of ice stream and ice shelf dynamics are required to contextualize modern change.

The offshore geomorphological imprint of ice streams and long-term grounding line retreat is relatively well established (Batchelor & Dowdeswell, 2015; Dowdeswell et al., 2020; Ó Cofaigh et al., 2002), but few studies have investigated the terrestrial geomorphological imprint of topographically constrained ice stream thinning, grounding line retreat and ice stream to ice shelf transition. Of the limited studies

executed to date, ice shelf advance and retreat history has been assessed using geomorphologic signals (England et al., 1978, 2009, 2022; Roberts et al., 2008; Sugden & Clapperton, 1981) or epishelf lake records (Antoniades et al., 2011; Bentley et al., 2005; Roberts et al., 2008; Smith et al., 2006). In addition, several studies in Antarctica have attempted to constrain Holocene rates of ice shelf thinning and retreat using surface exposure dating (e.g., Johnson et al., 2014; Mackintosh et al., 2014).

In Greenland, the last ice shelves fronting the northeast Greenland ice stream (NEGIS; Figures 1 and 2) have started to change dramatically with the disintegration of the Zachariae Isstrøm ice shelf post 2000 CE and rapid thinning of the Nioghalvfjædsfjorden Glacier (79N) ice shelf due to increased sub-shelf inflow of warm ocean water (Schaffer et al., 2020) and surface melt (Mayer et al., 2018). The Early Holocene history of NEGIS also suggests the potential for ice shelf disintegration and rapid grounding line retreat (Bennike & Weidick, 2001; Bentley et al., 2022; Larsen et al., 2018; Smith et al., 2022). However, the dynamics of this Holocene lateral transition remain poorly characterized and the geomorphology of ice stream to ice shelf transitions remains largely unconstrained.

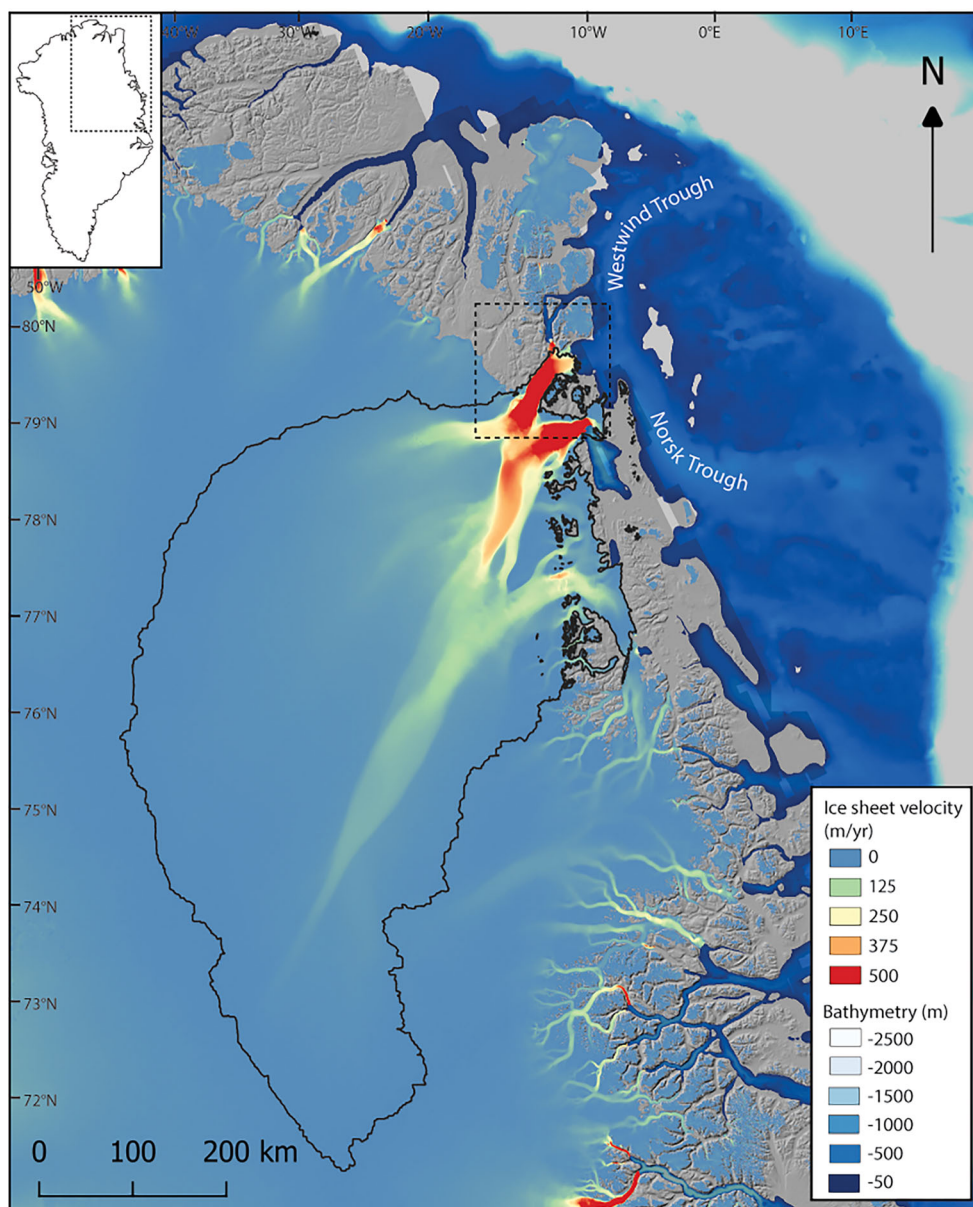


FIGURE 1 Overview of northeast Greenland, showing the NEGIS drainage basin (black solid line) and ice sheet velocity, generated using auto-RIFT (Gardner et al., 2018) and provided by the NASA MEaSUREs ITS_LIVE project (Gardner et al., 2019). Overlain on the ArcticDEM with IBCAO bathymetry (Jakobsson et al., 2020). Black dashed box shows location of Figure 2. Figure generated using QGreenland (Moon et al., 2021) [Color figure can be viewed at wileyonlinelibrary.com]

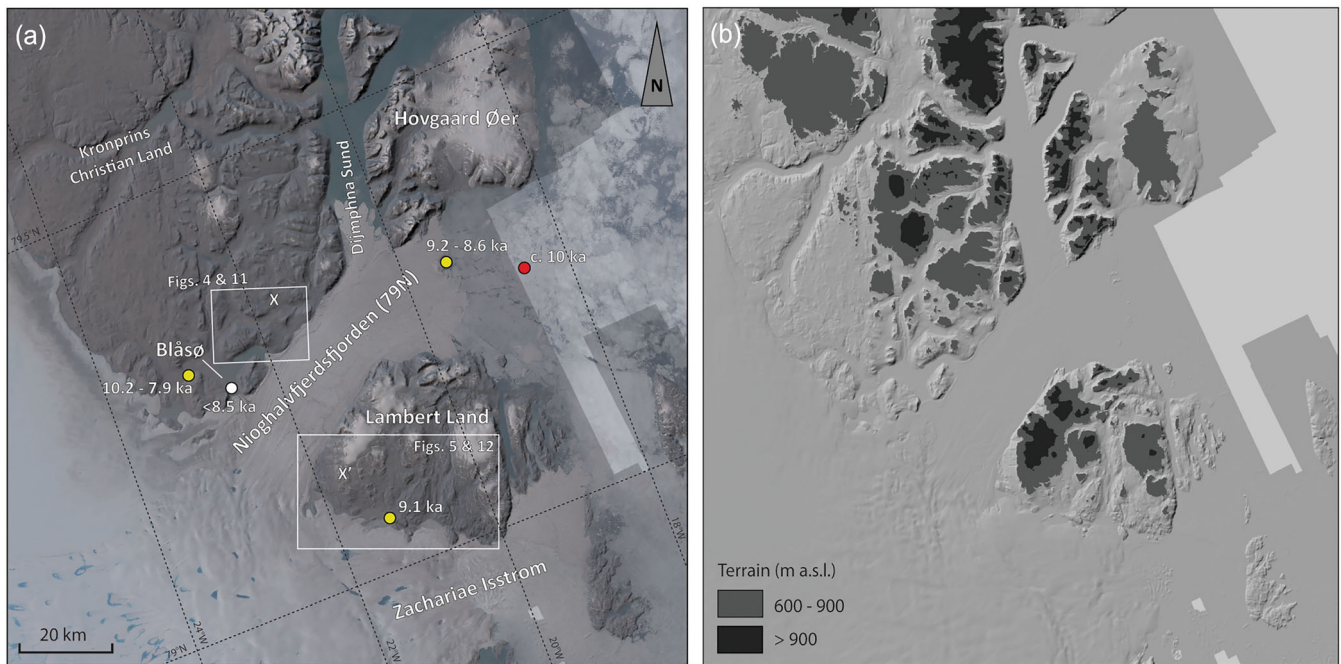


FIGURE 2 Map of the NEGIS region (a) localities mentioned in the text overlain on Sentinel-2 imagery (courtesy of the US Geological Survey). The location of marine core PS100-270VC (red circle), surface exposure ages (yellow circles, from Larsen et al., 2018), and radiocarbon ages (white circle, from Smith et al., 2022) are shown. X–X' are the location of the profile in Figure 13. (b) Digital elevation model of the region, with terrain above 900 m a.s.l. and 600–900 m a.s.l. shaded. These areas are broadly coincident with autochthonous and allochthonous blockfields respectively (Figure 3) [Color figure can be viewed at [wileyonlinelibrary.com](https://onlinelibrary.wiley.com)]

This article aims to investigate the terrestrial landsystem associated with a thinning and retreating ice stream-ice shelf system and develop a geomorphological model for deglaciation, during the Early Holocene, of the NEGIS and its northern most ice shelf (79N). It examines: (i) the Last Glacial Maximum (LGM) ice stream configuration and interaction between local cold-based ice and the ice stream margin; (ii) the geomorphological signal of ice stream marginal thinning, and (iii) evidence for ice stream to ice shelf lateral transition during both the Early and Late Holocene. Combining this evidence we present an integrated landsystem model for an ice stream to ice shelf transition that can be used to identify such transitional zones and the former presence of ice shelves in the geological record.

2 | PREVIOUS WORK

2.1 | Geomorphological records of ice streams and ice shelves

The geomorphological imprint of Arctic and Antarctic ice streams and ice shelves has been studied remotely and in the field for several decades. Contemporary ice shelves remain critical, fringing 75% of the Antarctic coastline (Rignot et al., 2013), whereas only a few large ice shelves and ice tongues now remain in the Arctic (Dowdeswell & Jeffries, 2017).

2.1.1 | Antarctic

Offshore geomorphology provides the clearest expression of former ice stream expansion and retreat in Antarctica. Geomorphology

mapped from high-resolution swath bathymetry has formed the basis of landsystem models used for identifying and interpreting previously unconstrained ice stream and ice shelf dynamics (Andreassen et al., 2014; Graham et al., 2009; Ó Cofaigh et al., 2008).

While investigations of onshore, terrestrial ice stream and ice shelf geomorphology are limited, they have provided theoretical models for understanding ice shelf dynamics. Grounded ice along the margins of George VI Ice Shelf, abutting Alexander Island, created distinctive ice-cored moraines thought to have been formed by thrusting and ablation of debris-rich ice (Sugden & Clapperton, 1981). These landforms combine exotic, far-travelled sediments from the ice stream and reworked local material from the ice margin and sub-ice shelf. Hambrey et al. (2015) invoked 'controlled' moraine formation (Evans, 2009) relating to the structural glaciology of George VI ice shelf, with linear accumulations of ice cored sediment controlled by longitudinal foliation. Subsequently, Davies et al. (2017) found close vertical association of lateral moraines, ice shelf moraines and epishelf lakes (a lake which is impounded in an ice free depression or embayment by an ice shelf or glacier, and is connected to the marine environment [cf. Gibson & Andersen, 2002]), linked with the transition from an ice stream to the George VI Ice Shelf at some point following the LGM. In contrast, on McMurdo Ice Shelf, ice shelf moraines were formed supraglacially, through the release of accreted subglacial sediment entrained into the ice shelf via basal freeze-on of marine waters (Glasser et al., 2006). Fresh water and tidal (epishelf) lakes are also important components of the ice shelf landsystem and sediment records from such lakes have been utilized to constrain reconstructions of ice shelf growth and decay through time (Roberts et al., 2008; Smith et al., 2006, 2007).

2.1.2 | Arctic

Many studies have used glacial geomorphology to reconstruct palaeo-ice streams in Canada, Greenland, and Fennoscandia (e.g., Freire et al., 2015; Lane et al., 2014; Newton et al., 2017; Ó Cofaigh et al., 2013; Roberts et al., 2010, 2013; Stokes & Clark, 2003), and there are limited observations of streamlined bedforms evolving beneath contemporary ice streams (Jakobshavn Isbrae: Jezek et al., 2011, NEGIS: Franke et al., 2020). However, due to the current paucity of Northern Hemisphere ice shelves, few studies have examined Arctic ice stream–ice shelf landsystems (Furze et al., 2018).

Marine evidence suggests that ice streams terminating in floating ice shelves preferentially produce grounding-zone wedges, whereas tidewater margins result in moraine formation (Batchelor & Dowdeswell, 2015; Dowdeswell & Fugelli, 2012). On Ellesmere Island, in the Canadian High Arctic, an abrupt transition of lateral moraines and conical kames to horizontal moraines has been used as evidence of past grounding line position and former presence of an ice shelf (England et al., 1978). The moraines were associated with large, fossiliferous proglacial terraces composed of till, ice-rafted debris, and outwash sands, representing a period of ice shelf retreat. Hodgson and Vincent (1984) also reported ice shelf moraines and associated tills deposited up to the marine limit around Viscount Melville Sound in the Canadian High Arctic. Till deposition by the ice shelf was associated with striae and ice marginal fluvial landforms. In the same area, England et al. (2009) noted glaciotectonism of epishelf lake sediments associated with the ice shelf, indicative of marginal glaciofluvial activity. In north Norway, Evans et al. (2002) reported multiple bouldery ice shelf moraines in fjords that contained outlet glaciers during the late glacial, linked to ice shelf migration. In Baffin Bay, offshore swath bathymetry and seismic data revealed large lateral ice shelf moraines, providing evidence for a 500 m thick ice shelf in northern Baffin Bay during the LGM (Couette et al., 2022).

In north Greenland, Larsen et al. (2010) and Möller et al. (2010) described geomorphological evidence for a large, regional ice shelf that flowed east from the Nares Strait along the north Greenland coast. This ice shelf was grounded onshore, depositing a sub-ice shelf till and impounding ice marginal lakes against its southern margin. Glaciolacustrine and glaciofluvial kame sediments deposited above the marine limit record ice shelf presence, prior to deglaciation and the deposition of marine sediments across lower elevations. Preserved dead-ice terrain also suggests burial of the ice shelf margin by marginal glaciofluvial activity during deglaciation. Raised marine deltas at valley mouths up to 40–45 m above sea level (a.s.l.) reflect a marine transgression at 10.1 ka following deglaciation (Larsen et al., 2010).

2.2 | NEGIS and Nioghalvfjordsfjorden Glacier

NEGIS is the largest ice stream in Greenland, draining ~12% of the ice sheet (Figure 1; Fahnestock et al., 1993; Joughin et al., 2010). The ice stream branches into three outlet glaciers: Nioghalvfjordsfjorden Glacier (79N), Zachariae Isstrøm (ZI) and Storstrommen. 79N is the only ice stream with a contemporary buttressing ice shelf. The ZI ice shelf disintegrated after 2010 to leave a grounded tidewater margin. The retreat and disintegration of the ZI ice shelf has been linked to both increased air temperatures and sea ice loss (Khan et al., 2014), and increased submarine melt following the ingress of warm Atlantic water (Mouginot et al., 2015; Schaffer et al., 2020). It is thought that

ZI will be highly unstable over the coming decades due to sustained high submarine melt rates and a proximal bed over-deepening (Choi et al., 2017). In contrast, 79N is currently predicted to remain relatively stable for the rest of the century, due to the stabilizing effect of ice rises and bedrock island (Choi et al., 2017). The present 79N ice stream and ice shelf are confined to Nioghalvfjordsfjorden between Kronprins Christian Land to the north and Lambert Land to the south. Higher-elevation terrain is covered in places by local plateau ice caps, mostly on Hovgaard Øer and Lambert Land (Figure 2).

The geomorphology within Westwind and Norske Troughs (Figure 1) have been used to reconstruct the former offshore extent of the palaeo-ice stream. Ice stream subglacial landforms such as mega-scale glacial lineations, lateral shear moraines, grounding zone wedges, and De Geer moraines show that the palaeo-ice stream reached the continental shelf break, most likely at the LGM although these landforms are undated (Arndt et al., 2015, 2017; Batchelor & Dowdeswell, 2016; Evans et al., 2009; Winkelmann et al., 2010). Timing of the initial retreat across the NEGIS outer continental shelf remains uncertain, but occurred between 13.4–12.5 ka BP, driven by an influx of Atlantic Water (Davies et al., 2022). The ice shelf margin then remained close to the inner continental shelf until 11.2–10.8 ka BP, before retreating westwards (Arndt et al., 2017; Davies et al., 2022). Concomitant rates and patterns of ice thinning across the coastal mountains during early deglaciation are unconstrained, despite their importance for numerical model validation. The ice terminus reached the outer coast by ~11.5 ka and retreated to the inner coast by ~10.0–9.0 ka, (Figure 2; Larsen et al., 2018) This accords with marine biomarker evidence for ice shelf disintegration and NEGIS grounding line retreat to just east of Hovgaard Øer by c. 10.0 ka (west of core site PS100-270VC; Figure 2; Syring et al., 2020). Evidence for further retreat is constrained by exposure ages of 9.2–7.9 ka west of Blåså and 9.1–9.0 ka on the south coast of Lambert Land (Figure 2; Larsen et al., 2018). Radiocarbon dates from Blåså suggest that the ice shelf retreated between 8.5 and 4.4 ka BP (Smith et al., 2022). This is supported by radiocarbon ages on driftwood and whalebones from palaeo-shorelines which imply open water marine conditions within 79N fjord and Blåså between 7.0–5.4 cal ka BP (Bennike & Weidick, 2001). This was during the Holocene climatic optimum, an unusually warm period across much of the Arctic from roughly 8.0 to 5.0 ka (Kaufman et al., 2004), which led to extensive ice sheet thinning and retreat (Nielsen et al., 2018).

The location of the NEGIS grounding line between 7.8–1.2 ka is poorly constrained, but Larsen et al. (2018) estimate it was c. 20–70 km inland of its present position. The ice shelf is thought to have regrown after 4.4 cal ka BP, coincident with decreasing atmospheric temperatures, and an increase in Polar Water dominance (Smith et al., 2022), reaching its maximum extent during the Little Ice Age (LIA) (Bennike & Weidick, 2001).

3 | METHODS

In this study we focussed on the terrain to the north of the 79N outlet (Kronprins Christian Land and Hovgaard Øer; Figure 2), and the large island to the south (Lambert Land; Figure 2). The locations were chosen for the well-preserved geomorphology, evident from satellite images, and accessibility. The study area was mapped using field and remote mapping. Initial reconnaissance prior to fieldwork was conducted in Google Earth Pro to identify landforms and areas of interest. Where

accessible in the field, these areas were targeted for detailed field mapping in 2017, which covered significant regions along the northern side of Nioghalvesfjorden between Blåsø and Hovgaard Øer. Remote and field mapping were combined to create a geomorphological map.

Landforms were mapped following Chandler et al. (2018), and the terrestrial landform map was produced using the QGreenland package (Moon et al., 2021) in QGIS 3.22. We identified landforms from Google Earth imagery (dominantly 2017-20 Maxar Technologies) and Landsat satellite imagery – overlain on SRTM and ArcticDEM (vertical accuracy of 2 m and horizontal resolution of 3.8 m). This allowed detailed mapping, and measurement of landform elevations, which are ellipsoidal heights from the ArcticDEM (roughly 30 m above geoidal heights). Ice shelf geomorphology mapping was undertaken separately in Esri ArcMap using ArcticDEM and Google Earth Pro. Ice surface velocity data was obtained from the MEaSUREs Greenland Ice Sheet Velocity Map and sub-shelf bathymetry and subglacial topography was taken from BedMachine version 3 (Morlighem et al., 2017). Ice

surface reconstructions were plotted using a 1° surface slope in line with the current ice sheet surface in this region.

4 | RESULTS

4.1 | Local glaciation

Local ice occurs at higher elevations to the west of the study area (> 800 m a.s.l.) and lower elevations closer to the coast in the east (> 500 m a.s.l.). Some plateau ice cap outlet glaciers extend down to sea level. The geomorphological imprint of local ice masses at higher elevations is limited, as past expansion has caused little erosion or deposition and evidence of meltwater drainage forming ice marginal channels is rare. Where outlets reached lower elevations (e.g., Hovgaard Øer) they formed arcuate, latero-terminal moraines, distinguishable from landforms formed by the ice shelf margin based on their orientation and morphology.

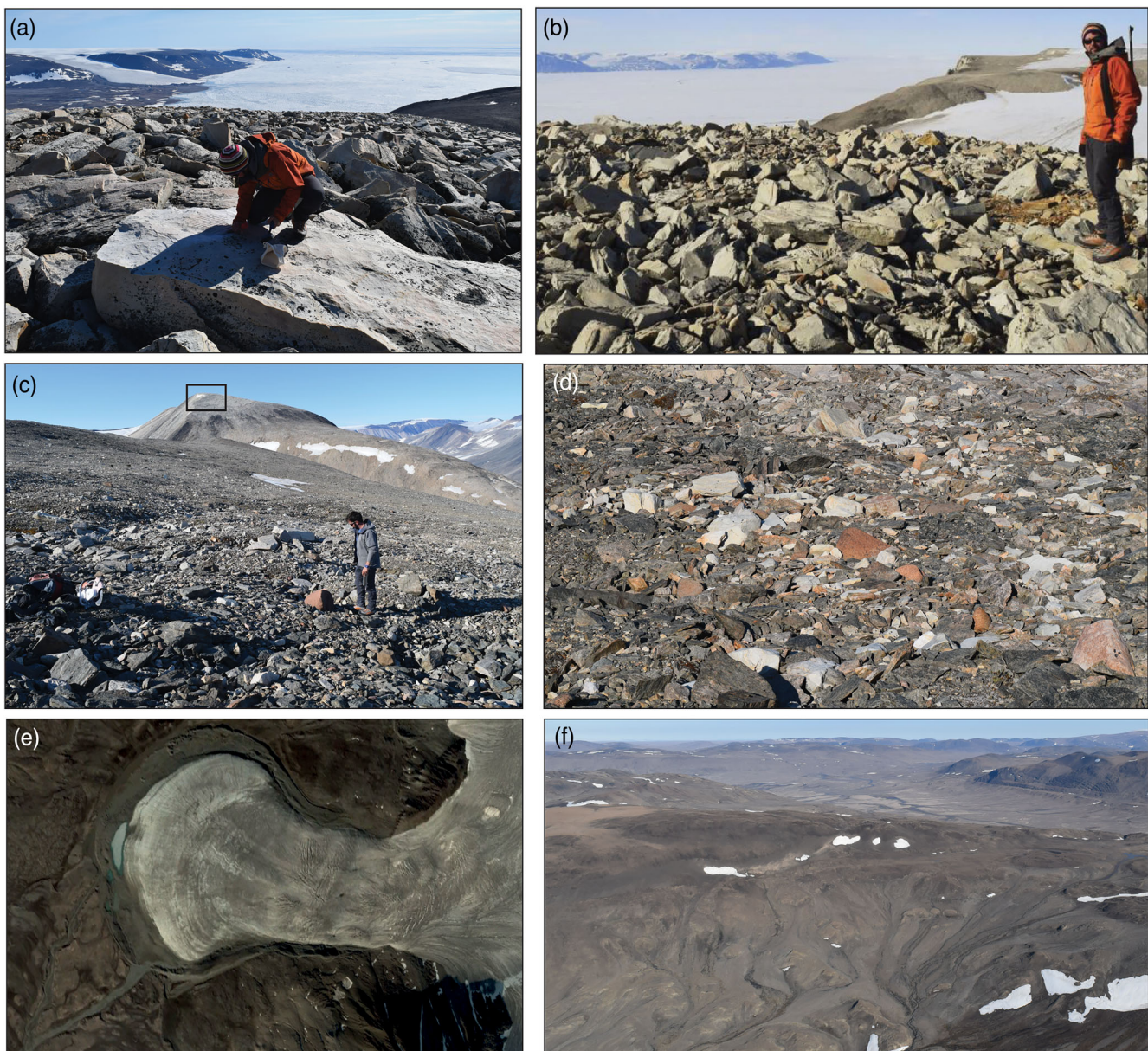


FIGURE 3 Blockfields on Hovgaard Øer. (a, b) Autochthonous blockfield at ~ 1000 m a.s.l. (c, d) lower elevation (~ 650 m a.s.l.) allochthonous blockfield with common orange-brown sandstone erratics. Black box in (c) shows the location of (a) and (b). (e) Local ice mass on Hovgaard Øer with clear arcuate latero-terminal moraines. (f) Oblique aerial photograph of the allochthonous blockfield east of Blåsø, showing clear debris stripes and evidence for gelifluction [Color figure can be viewed at [wileyonlinelibrary.com](https://onlinelibrary.wiley.com)]

4.2 | Blockfields

Autochthonous blockfields are common at elevations above ~ 900 m a.s.l. On Hovgaard Øer they extend continuously over hundreds of vertical metres and consist of clast-supported, angular to very angular blocks of local quartzite bedrock with no erratics (Figure 3a,b). Most boulders are less than 1 m (*a*-axis), with some larger exceptions reaching up to 3 m (*a*-axis). The autochthonous blockfields transition downslope to matrix-supported allochthonous blockfields between 900 and 600 m a.s.l. and contain both local quartzite and far-travelled erratics (e.g. sandstone, limestone, conglomerate: Figure 3c,d). The allochthonous blockfields can be traced away from plateau summits, draping the landscape downslope with signs of movement via gelifluction (see Fig. 3f). Indeed, evidence for periglacial processes is widespread in the form of patterned ground, debris stripes and gelifluction lobes. These high-elevation, autochthonous blockfields above ~ 900 m a.s.l. are interpreted as *in situ* regolith, indicating little or no glacial erosion over extended time periods (10s–100s ka; Rea et al., 1996, Ballantyne, 2018).

Between ~ 600 –0 m a.s.l. along the northern margins of 79N fjord, the terrain continues to be dominated by allochthonous blockfields and sediments reworked by slope processes, but with a noticeably higher quantity of glacially-abraded erratics. The landscape at this elevation is interspersed with localized (< 1 km²) outcrops of glacially abraded bedrock, typically below 200 m a.s.l. on promontories projecting into the fjord (e.g., southern coast of Hovgaard Øer), displaying striations and perched erratic boulders. The presence of erratic boulders on allochthonous blockfield slopes between 900 and 600 m a.s.l. is clear evidence for past ice cover.

4.3 | Ice stream geomorphology

4.3.1 | Moraine ridges

Moraines are common between 600 and 200 m a.s.l. along the northern side of 79N fjord (Figure 4), and the southern edge of Lambert

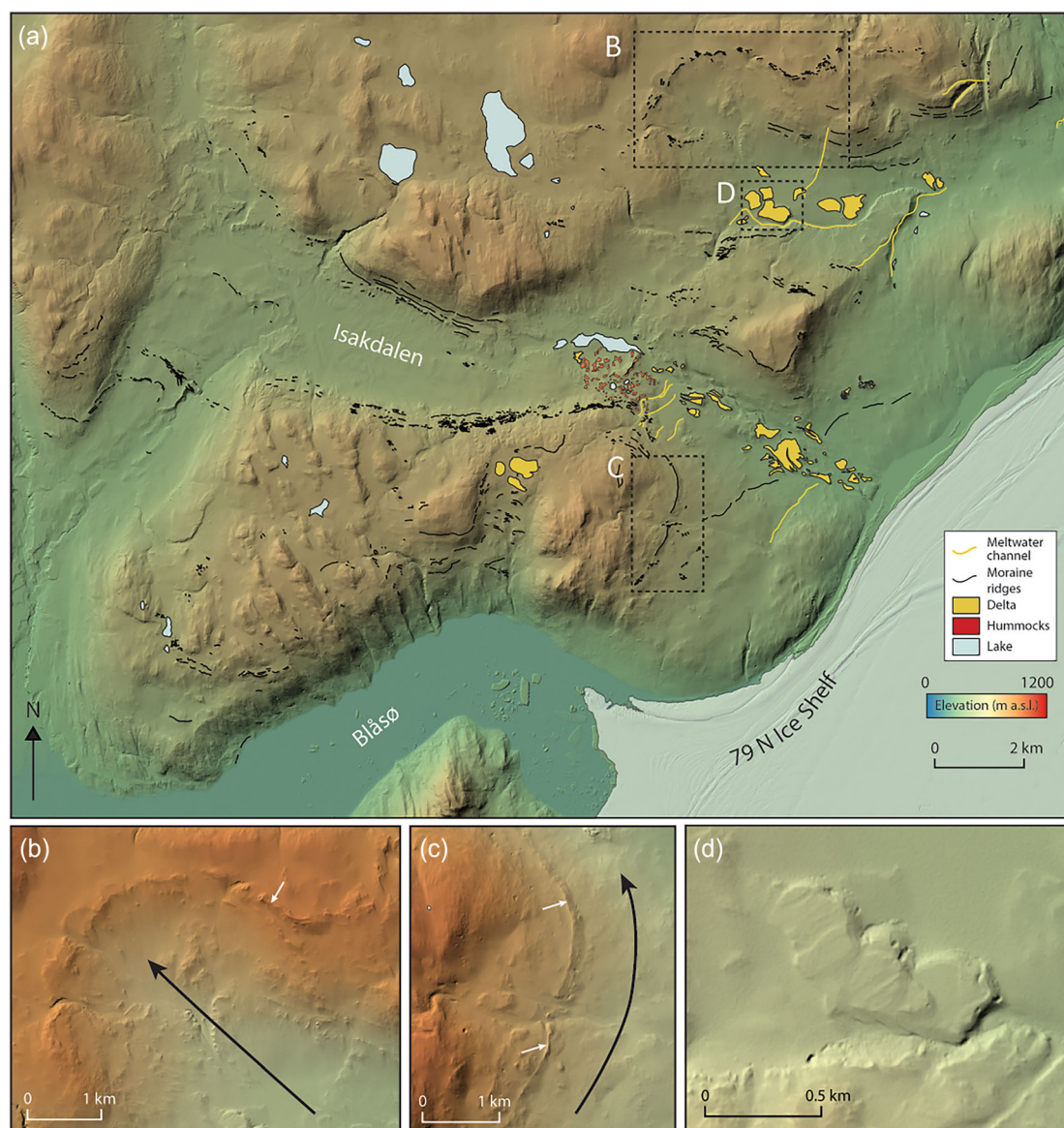


FIGURE 4 Glacial geomorphology northeast of Blåsø (location shown on Figure 2). (a) Geomorphological map of the northern 79N region; (b) high elevation (c. 600 m a.s.l.) latero-terminal moraine; (c) lateral moraine which continues from Blåsø to Isakdalen; (d) one of the delta staircases. Arrows in (b) and (c) indicate inferred palaeo ice flow direction. Mapping overlain on ArcticDEM, generated using QGreenland (Moon et al., 2021). White arrows in (b) and (c) indicate the location of the moraine ridges [Color figure can be viewed at [wileyonlinelibrary.com](https://onlinelibrary.wiley.com/terms-and-conditions)]

FIGURE 5 (a) Glacial geomorphology of the southwest coast of Lambert Land (location shown on Figure 2).

Contemporary 79N ice is shown by white shading. Black lines denote lateral moraine staircases, yellow polygons mark individual deltas and delta staircases. There are also ice marginal channels (yellow lines) which often run sub-parallel to lateral moraines. (b, c) Satellite images showing examples of ice marginal channels found in the study area [Color figure can be viewed at wileyonlinelibrary.com]

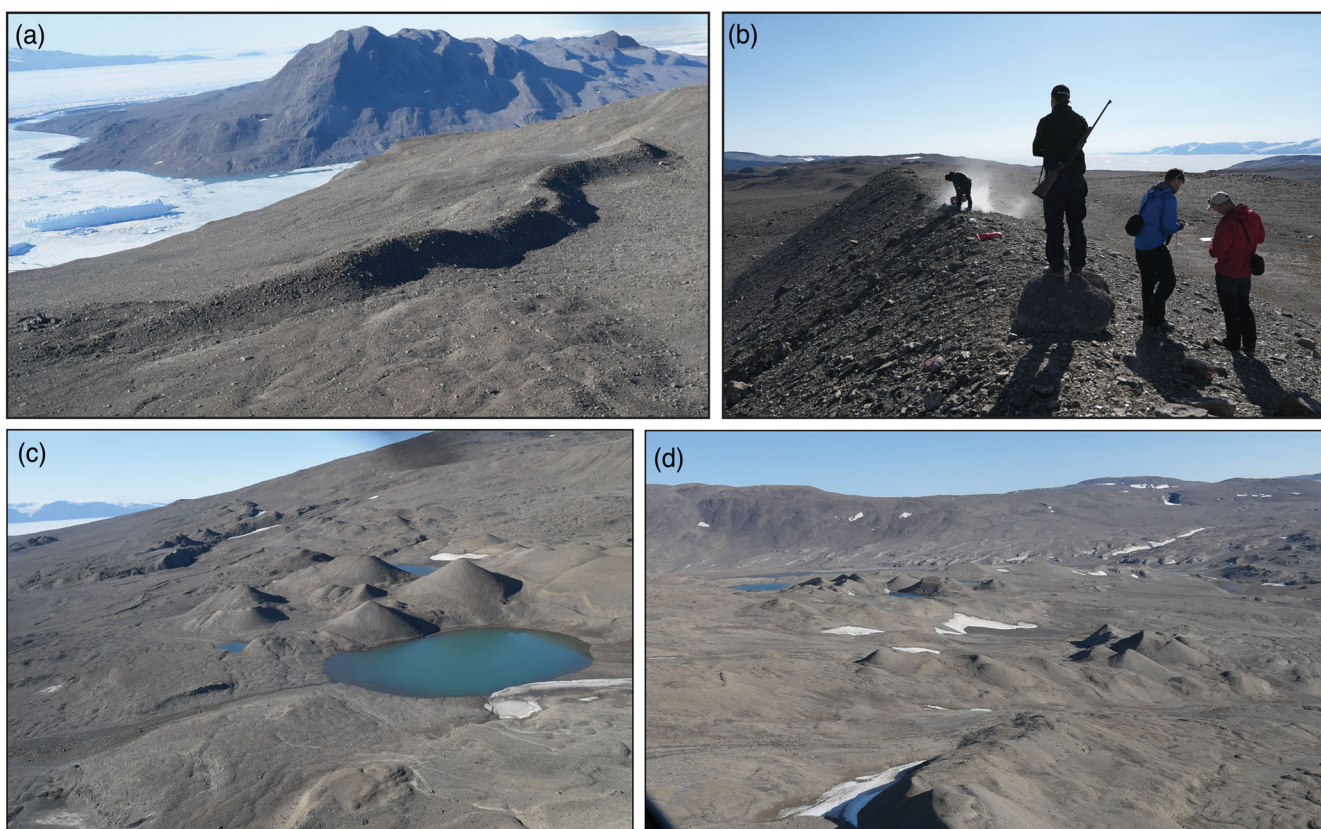
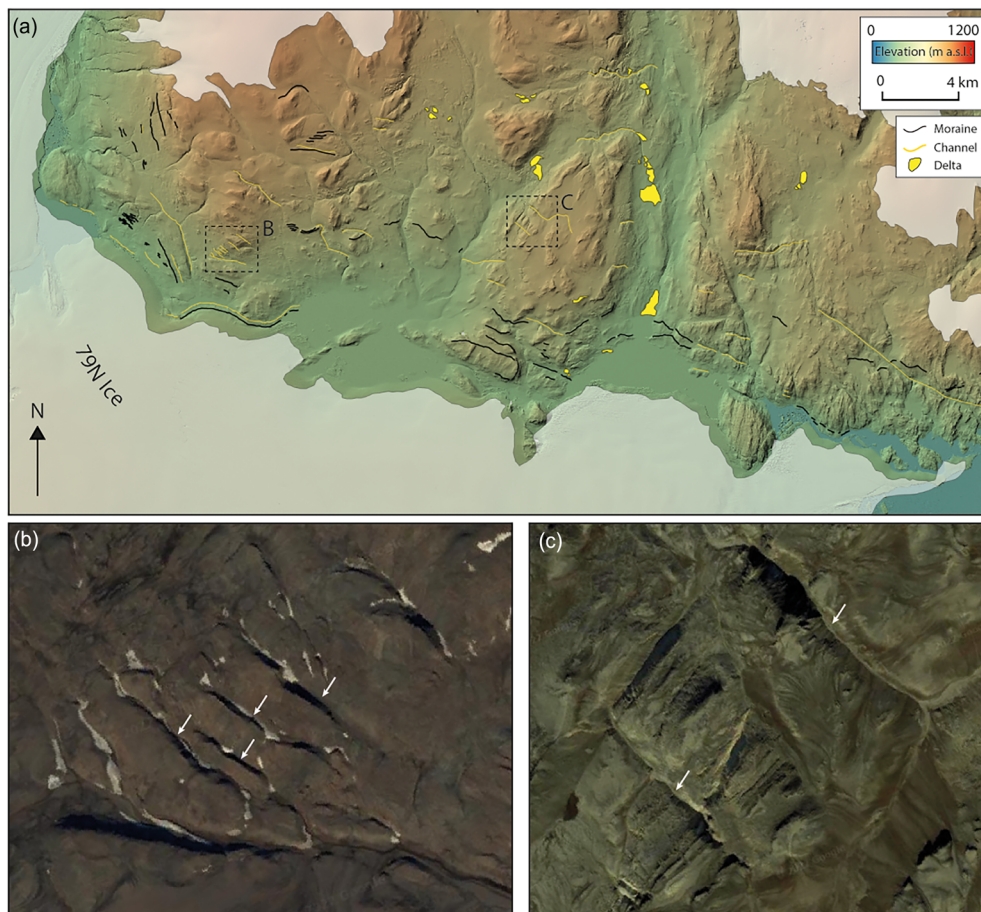


FIGURE 6 (a) Oblique aerial and (b) crest-top photographs of the highest elevation ice stream moraine mapped in the study (box B in Figure 4a). (c, d) Oblique aerial photographs of 'hummocky' terrain showing conical mounds and circular pools, located at the eastern end of Isakdalen (see Figure 4a for location) [Color figure can be viewed at wileyonlinelibrary.com]

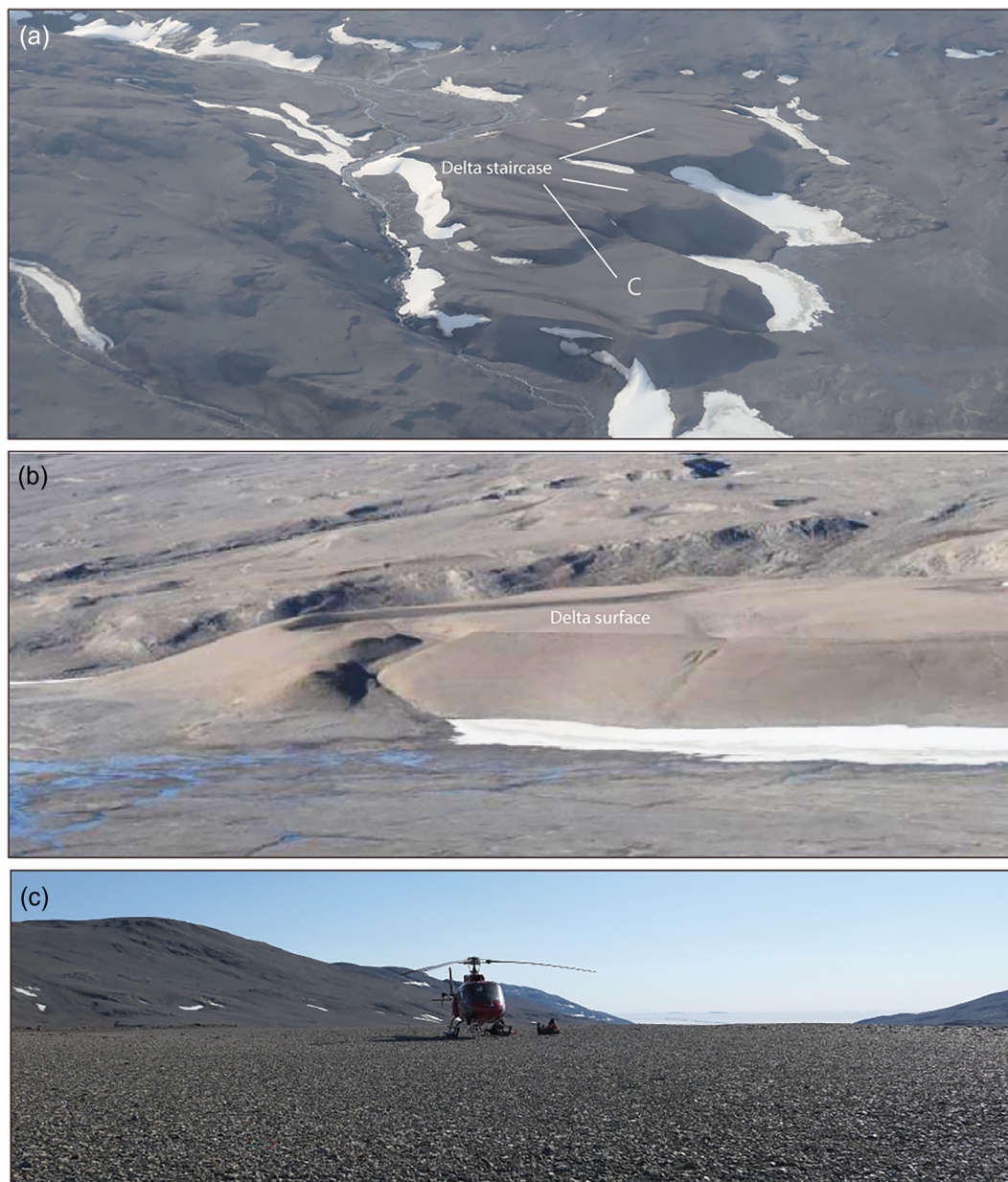


FIGURE 7 (a, b) Oblique aerial and (c) ground-level photographs of a delta staircases (see Figure 4a,d for location). Photograph (c) is taken from the lowest delta surface seen in (a) [Color figure can be viewed at [wileyonlinelibrary.com](https://onlinelibrary.wiley.com/terms-and-conditions)]

Land (Figure 5). They are characterized by distinctive arcuate lateral ridges (Figure 6a,b) and ‘hummocky’ moraine complexes (Figure 6c,d). In some cases, moraines are nested, often linked to raised deltas (Figure 7). One of the clearest examples of an arcuate, single-crested moraine runs roughly northwest–southeast (NW–SE), skirting a broad valley for over 6 km at 600–580 m a.s.l. (79.692°N, 21.476°W), (Figures 4a,b and 6a,b). The ridge is more than 10 m high and consists of unconsolidated diamict ranging from silt to boulders of varying lithologies. Occasional boulders up to a metre in diameter were observed. Nested lateral moraines occur within marginal valleys and cols adjacent to the 79N fjord, most commonly between 450 and 300 m a.s.l. but also evident down to ~200 m a.s.l. The clearest examples are found on both the northern and southern sides of Isakdalen (informal name) – northeast of Blåsø – from 430 to 320 m a.s.l. (Figure 4a). These moraines are 5–8 m high, up to 20 m wide, and composed of unconsolidated diamict with mixed lithologies. Ridge crests are often sub-horizontal where intact, but many are heavily degraded downslope by periglacial activity. Together these are

interpreted as lateral or terminal moraine, recording previous ice sheet extent (Benn & Evans, 2014).

In some locations arcuate moraine ridges fragment into zones of distinctive ‘hummocky’ moraine. These zones comprise broad chains of linear to conical ridges composed of partially sorted sediment and interspersed with kettle holes (Figure 6c,d). Occasionally they have flat upper surfaces. The best examples of these are found in the east of Isakdalen (Figure 4a), at an interfluvium between Isakdalen and the 79N fjord. In cross profile, conical moraines have steep proximal and distal sides with high angles of repose (Figure 6c,d). These are interpreted as ‘hummocky’ moraine, formed through ice-stagnation (Benn, 1992; Benn & Evans, 2014).

4.3.2 | Deltas

Perched deltas occur between 520 and 55 m a.s.l. on the northern 79N fjord wall, the south of Hovgaard Øer (Figure 4a) and Lambert Land

FIGURE 8 Photographs of glacially abraded bedrock surfaces on the south of Hovgaard Øer. A thin, layer of coarse till is visible between areas of exposed bedrock, along with common glacially transported erratics. Striae direction is shown by the white arrow in (a) [Color figure can be viewed at wileyonlinelibrary.com]

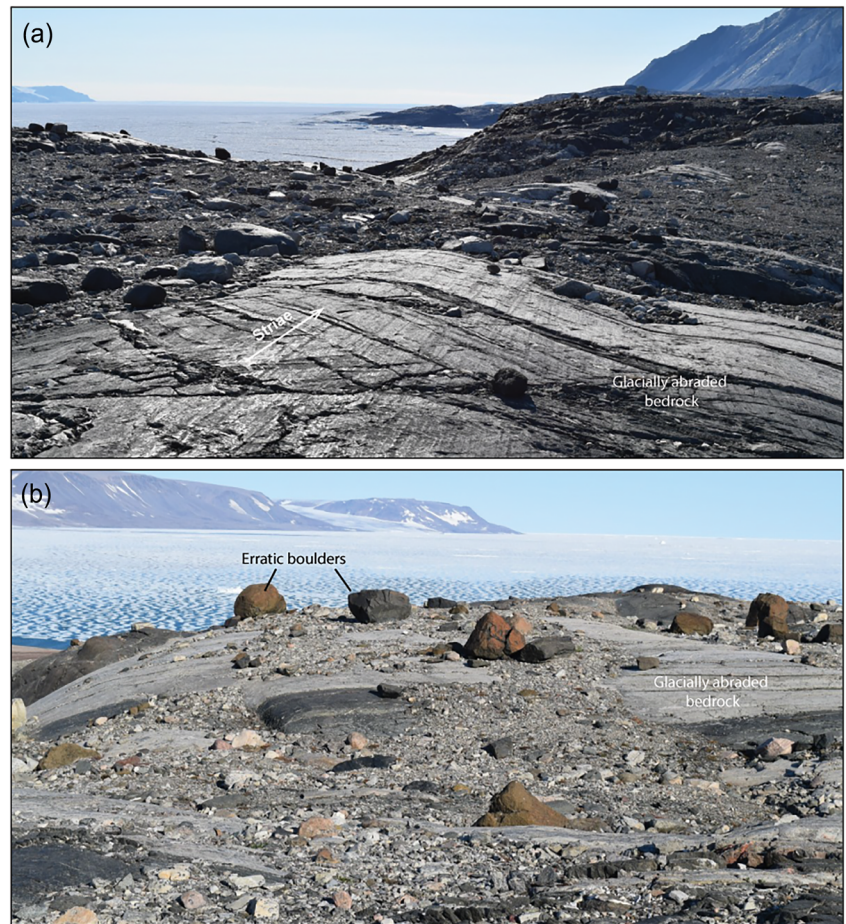


(Figure 5a). There are isolated examples, but they commonly occur in sets of altitudinally-zoned ‘staircases’ within marginal valleys. Many appear pristine, with smooth, gently grading tops, sharply defined ice-proximal slopes, and well-preserved lateral drainage channels (Figure 7). The deltas are composed of well-sorted glaciofluvial sediments from silts, through sands to cobbles. Some have been fragmented due to periglacial disturbance including the development of ice wedge polygons.

Large deltas are particularly prevalent in a discontinuous, NW–SE staircase on the floor of Isakdalen, leading down to the northern side of the 79N fjord (Figure 4a). The highest of these deltas is at ~300 m a.s.l. and closely associated with ‘hummocky’ moraine at 79.645°N, 21.785°W. The staircase is long (5.5 km) and narrow (0.7 km) and can be traced downslope, towards the south-east to ~50 m a.s.l. (Figure 4a). Further east, another delta complex is associated with streamlined, fluted glacial sediment that extends downslope of the delta and a former ice margin denoted by a clear drift limit. Their geomorphology and location suggest they are deltas, formed in either a glacier-fed or ice-contact setting (Benn & Evans, 2014).

4.3.3 | Channels

Bedrock- and sediment-incised channels run across valley slopes and most commonly sub-parallel to lateral moraines. Bedrock-incised channels are short (< 1 km) and steep, and relatively deep (approximately 50–10 m), and occasionally cut across local watersheds. These

appear to be overspill channels, formed through water overspill and incision following ice damming (Lane et al., 2015a). In contrast, channels that run sub-parallel to lateral moraine ridges are generally shallower with lower gradients and are often nested. In some cases, they occur at the transition between lateral and ‘hummocky’ moraine, such as at Isakdalen (Figure 4) and on the south-western slopes of Lambert Land (Figure 5). These are interpreted as lateral meltwater channels (Kleman et al., 1997).

4.3.4 | Streamlined terrain

Allochthonous blockfields drape the landscape adjacent to the northern edge of the 79N fjord at 900–600 m a.s.l. Bedrock outcrops appear between 600 and 400 m a.s.l., showing some limited evidence of smoothing and striations although surfaces are not heavily abraded. Below 400 m a.s.l., bedrock is heavily abraded and scoured along the fjord walls (Figure 8), particularly towards the east on the lower, south-facing flanks of Hovgaard Øer. Here, gneissic bedrock has been abraded and plucked to form whalebacks and roches moutonnées (Figure 8b). Striae are orientated west–east, and plucked faces are found on the east side of roches moutonnées, consistent with eastwards ice flow. There are erratic boulders of mixed lithology (e.g., quartz, quartzite, conglomerate, sandstone, limestone) scattered across the surface of scoured bedrock. Abraded bedrock outcrops with frequent perched boulders were also found further up-fjord, at the western end of Blåsø, from 600 to 100 m a.s.l.

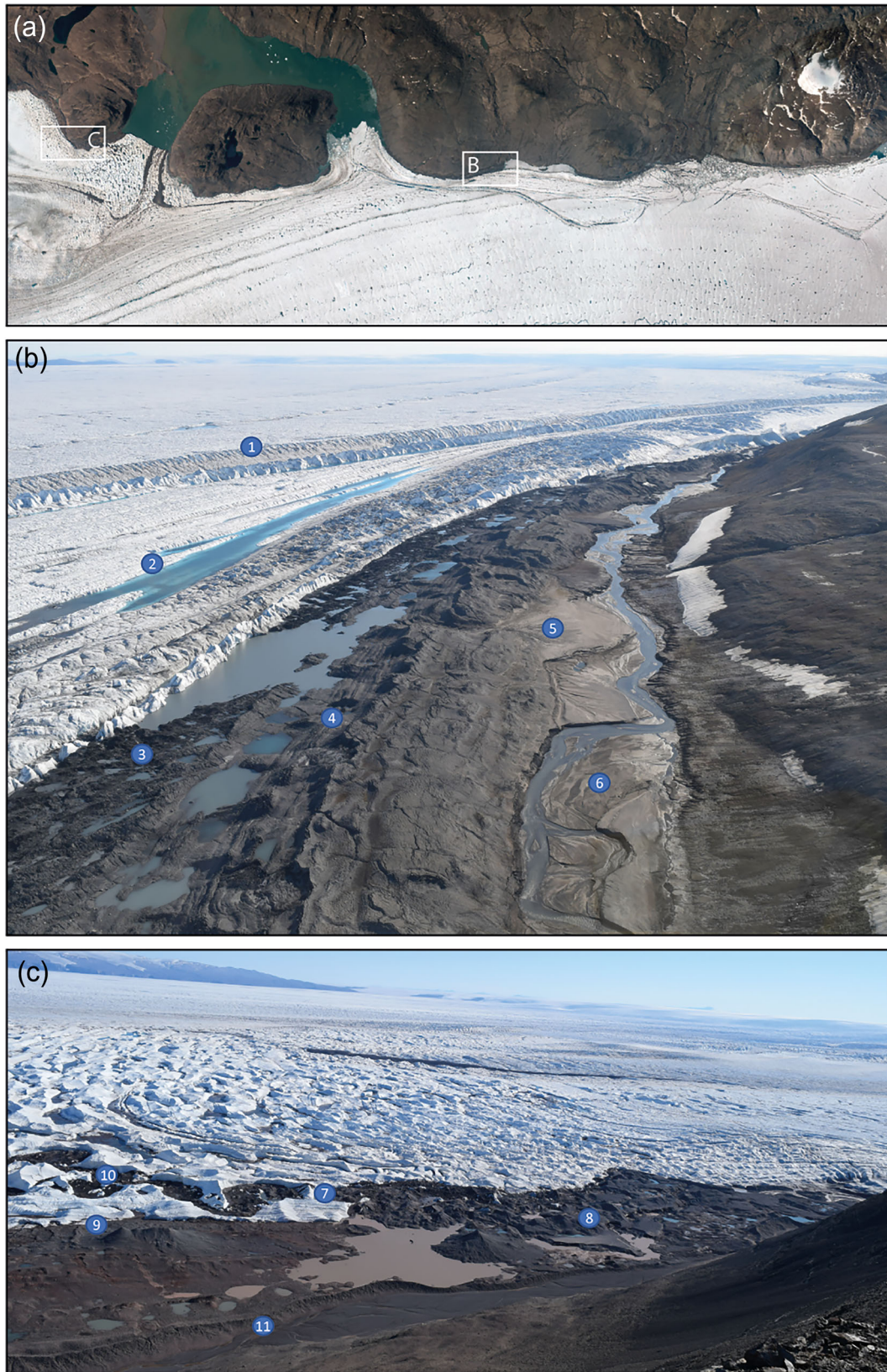


FIGURE 9 (a) Overview of the northern margin 79N ice shelf. (b) Oblique aerial photograph showing ice shelf geomorphology mid-79N fjord. Note: (1) Midgardsommen ridge; (2) linear and ovate supraglacial drainage controlled by longitudinal foliation in the ice shelf; (3) burial of ice shelf margin by fluvio-glacial sediment/development of ice stagnation topography and localized ponding; (4) linear ridges; (5) outwash fans; (6) braided fluvio-glacial corridors forming kame terraces. (c) Oblique aerial photograph showing ice shelf geomorphology west of Blåsjø. Note: (7) longitudinal foliation exposed in section along the grounded ice shelf margin; (8) braided outwash surfaces; (9) crevasses infills; (10) supraglacial fluvial corridor; 1(1) the Little Ice Age shelf moraine impounding marginal lakes [Color figure can be viewed at [wileyonlinelibrary.com](https://onlinelibrary.wiley.com/terms-and-conditions)]

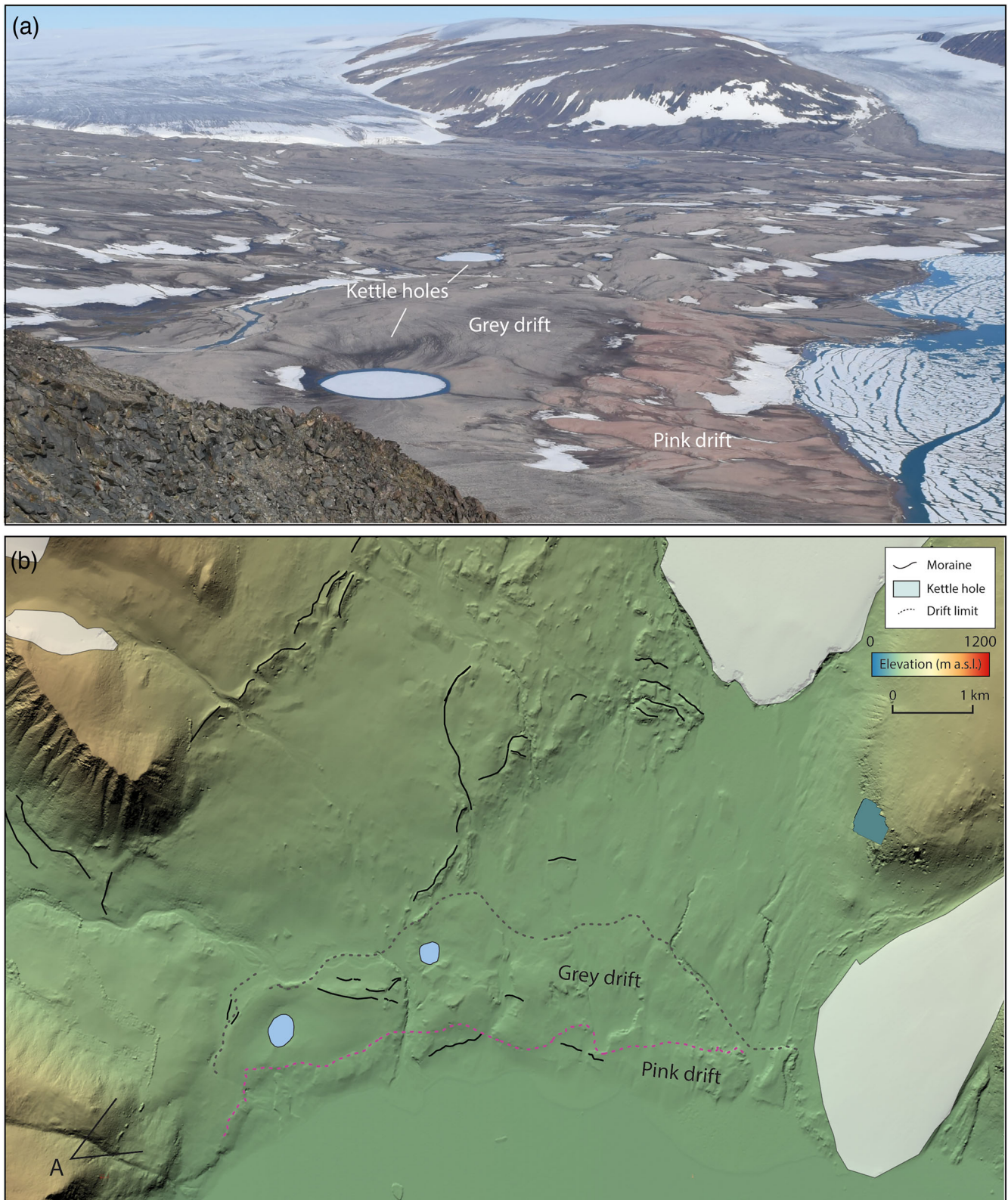


FIGURE 10 (a) Photograph looking over the southern coast of Hovgaard Øer, showing pink and grey drift, and kettle holes. Photograph location shown in (b). (b) Glacial geomorphology from the south coast of Hovgaard Øer, overlain on ArcticDEM [Color figure can be viewed at [wileyonlinelibrary.com](https://onlinelibrary.wiley.com/terms-and-conditions)]

4.4 | Ice shelf geomorphology

4.4.1 | Ice-marginal linear ridges

A complex of nested, linear ridges runs intermittently for over 40 km sub-parallel to the northwest margin of the 79N ice shelf (Figure 9). These are all at low elevation (< 30 m a.s.l.) with the largest, outer ridges sharply-defined, 5–10 m high and up to 10 m wide. Inboard of

the larger ridges are a series of smaller linear ridges < 5 m in height and width, forming an inset sequence of up to approximately 20 ridges between the outer limit and the present ice shelf margin. Active fluvial channels and lakes occur on the distal side of the ridges (Figure 9b) and, where the ridges are breached, small fan systems have formed. On the ice proximal side of the ridges, a band of debris-covered ice up to a few hundred metres wide forms actively down-wasting terrain within which the sediment is being reworked by glaciofluvial

processes (Figure 9a,b). To the west of Blåsø, exposures within outer linear ridges were found to be composed of reworked and folded marine shell-bearing muds. These linear ridges formed asymmetrically stacked sequences of deformed sediment emplaced over exposed bedrock.

On the southern coast of Hovgaard Øer, a series of degraded lateral moraines and ice-marginal lakes occur at ~400–60 m a.s.l. (Figure 10). At ~65 m a.s.l. (the local marine limit) a distinctive, grey-coloured glacial drift forms a lobate margin composed of a series of fragmented flat surfaces containing distinctive kettle holes. Overprinting this terrain is a second lobate margin composed of pink-coloured drift running adjacent to the coast at ~10 m a.s.l. The pink-coloured sediments are also heavily degraded but have fragmented linear ridges running west–east that lie sub-parallel to the coast.

4.4.2 | Transverse ridges

Transverse ridges running obliquely into the ice-marginal linear ridges are ubiquitous in the mid-fjord area, adjacent to the current northern edge of the ice shelf margin (Figure 9a). These landforms vary from arcuate to straight in planform but can be partially sinuous and crenulated in short sections. Sub-sets of ridges also run at opposing oblique angles to one another. In many localities they mimic the tensional crevasse patterns observed on the adjacent ice shelf.

4.4.3 | Ice-marginal and epishelf lakes

Many of the larger ice-marginal linear ridges impound small lakes adjacent to high ground. The lakes are generally linear or ovate in planform (Figure 9b,c), often forming a series of ribbon lakes. Multiple shorelines associated with these lakes record fluctuating water levels and perched lake sediment sequences were observed to contain laminated silts and muds with occasional dropstones. Some small lakes are impounded directly between the debris-free ice-shelf edge and the steep sides of the 79N fjord. In places, lakes have drained via overspill channels. Epishelf lakes, which have a direct connection to marine water under the ice shelf, are likely found along the edge of the ice shelf, but only in Blåsø is there direct observational evidence of a tidal marine influence (Bentley et al., 2022).

4.4.4 | Present-day ice shelf-marginal channels

Glaciofluvial sediments are common along the ice shelf margin. Corridors of channelized glaciofluvial sediments are clearly observed along the northern side of 79N with some channels being highly sinuous and mirroring supraglacial channels on the adjacent ice-shelf surface (Figure 9b). Elsewhere, channel systems are shallow and braided adjacent to the ice-shelf margin and beyond the LIA maximum limit. Sedimentation associated with these channels has partially buried the ice shelf margin in many places, resulting in fragmented, ice stagnation topography, with the development of kame and kettle topography, and sub-horizontal outwash surfaces interspersed with chaotic, dead-ice terrain (Figure 9b). A number of sinuous ridges may also be engorged eskers.

4.5 | Ice shelf structural glaciology

The north-western (NW) and south-eastern (SE) margins of the ice shelf contrast in terms of morphology and flow characteristics. Along the NW margin there are three unconstrained ice flow outlets from the ice shelf, one into each of the western and eastern ends of Blåsø, and one north into Dijnphna Sund (Figure 2). There are no inflowing glaciers downstream of the grounding line. In contrast, along the SE margin multiple ice field glaciers flow into the ice stream from Lambert Land, creating prominent flow units and there are no outlets. The front of the ice shelf abuts the small islands of Bloch Nunnatakker.

The contemporary ice shelf has several distinctive structural elements that provide insights into the geomorphological signal observed along the ice shelf margin. The ice shelf stretches a little over 70 km from the present grounding line and is, in places, greater than 20 km wide (Mouginot et al., 2015). The dominant features of the shelf are longitudinal, approximately flow-parallel features, which appear to be initiated proximal to the grounding line (Figure 9a). Given the presence of substantial annual surface melt, these features appear to be enhanced by channelling surface meltwater.

The ice which flows into the western side of Blåsø is sourced entirely from relatively slow moving ($< 100 \text{ ma}^{-1}$) grounded ice and appears to be partially grounded as it enters the epishelf lake (Bentley et al., 2022). ‘Midgardsormen’, which has been associated with compression in the ice shelf as it flowed obliquely across a lateral grounding line was described by (Mayer et al. 2018). It is no longer visible at the western entrance to Blåsø, suggesting the ice shelf no longer grounds in this manner at that location. Multiple Midgardsormen ridges can be seen along much of the rest of the NW margin, eastwards to Dijnphna Sund (Figure 9a,b) and as the ice shelf impinges on the southern shore of Hovgaard Øer. They are generally confined to within about 1 km inboard from, and are oriented sub-parallel to, the ice shelf lateral margin, but in a few locations, they angle obliquely towards the ice shelf. For the most part these appear in regions of the ice shelf calculated to be close to the floating-grounded marginal transition, by subtracting the elevation of the ice shelf base (assuming it is in hydrostatic equilibrium) from the bathymetry taken from Bed Machine version 3 (Bentley et al., 2022).

5 | DISCUSSION

5.1 | Evidence for local cold-based ice

The landscape we report surrounding 79N is typical of pan-North Atlantic glaciated continental margins. Substantial selective linear erosion by marine terminating ice streams results in deeply incised fjords separated by high elevation relict plateau surfaces (Kessler et al., 2008; Lane et al., 2016; Roberts et al., 2013; Sugden, 1974). Such plateaux host modern ice caps that are cold-based and – given the absence of significant erosional landforms or meltwater features on the plateaux – have likely experienced cold-based ice cover throughout much of the Quaternary, either from expanded local ice caps, or cold-based portions of the Greenland ice sheet. This difference in thermal regime is supported by inherited cosmogenic isotope signals on such Greenlandic plateau surfaces (Briner et al., 2014; Strunk et al., 2017). Elsewhere in Greenland, ice drawdown by ice

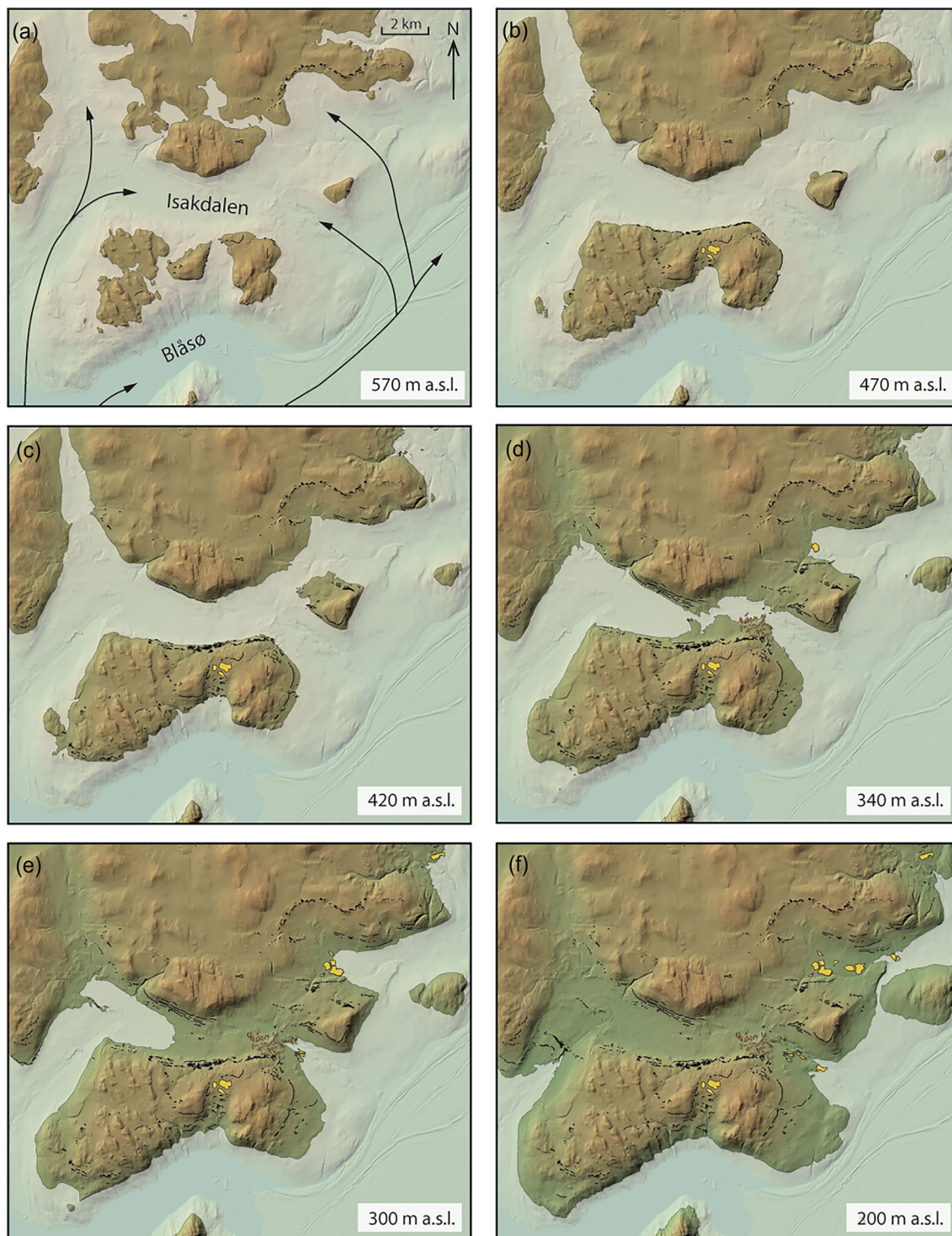


FIGURE 11 Elevational windows showing the inferred post-LGM thinning of the ice stream surface and geomorphology produced at each window in 79N. Arrows in (a) highlight inferred palaeo-ice flow directions, and extent is shown in Figure 2. Elevations refer to height of the ice stream margin above sea level. A 1° surface slope has been applied to the ice surface in these figures, similar to the currently observed ice surface slope of NEGIS. Geomorphological symbols are shown in Figure 4 [Color figure can be viewed at [wileyonlinelibrary.com](https://onlinelibrary.wiley.com/terms-and-conditions)]

streams in landscapes of selective linear erosion has been invoked as a means of starving peripheral high elevation plateaux of erosive ice (Beel et al., 2016; Lane et al., 2016; Roberts et al., 2013).

The high-elevation autochthonous blockfields are likely to have remained ice-free for much of the Quaternary and/or been periodically covered by thin, non-erosive ice (Strunk et al., 2017). Dual $^{10}\text{Be}/^{26}\text{Al}$ nuclide concentrations from bedrock and erratic samples at 900–500 m a.s.l. in Dove Bugt – south of the study area – highlight slow rates of plateau erosion since 0.6–1.0 Ma, although it is unclear for

what percentage of time autochthonous blockfields have been buried or exposed (Skov et al., 2020). It is also hypothesized that the slow erosion rates post 0.6 Ma mark the onset of accelerated ice sheet incision resulting in the development of overdeepened fjords, and the abandonment of ice sheet erosion of high-level surfaces (Skov et al., 2020).

Allochthonous blockfields are extensive between 900 and 600 m a.s.l., and provide clear evidence of past ice cover suggesting erratics were transported and deposited by cold-based ice that preserved the underlying periglacial landscape. Allochthonous blockfields

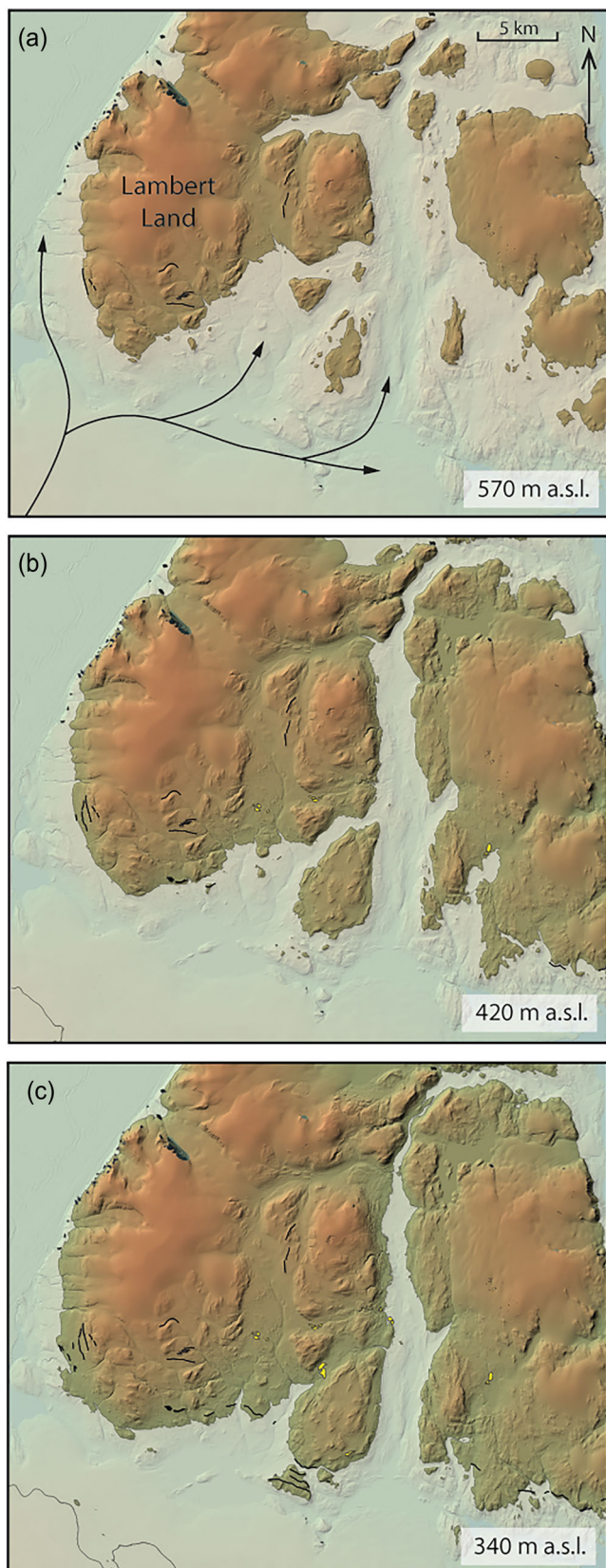


FIGURE 12 Elevational windows showing the inferred post-LGM thinning of the ice stream surface and geomorphology produced at each window on southern Lambert Land. Arrows in (a) highlight inferred palaeo-ice flow directions, and extent is shown in Figure 2. Elevations refer to height of the ice stream margin above sea level. A 1° surface slope has been applied to the ice surface in these figures, similar to the currently observed ice surface slope of NEGIS. Geomorphological symbols are shown in Figure 4 [Color figure can be viewed at wileyonlinelibrary.com]

can also form from old glacial material (Dahl, 1966), meaning it is possible that these areas developed slowly, from a Late Pliocene to Mid Pleistocene till cover, supporting the hypothesis of long-term fjord development highlighted by Skov et al. (2020).

Passive emplacement of erratics on blockfields is likely linked to a transition from warm- to cold-based ice within the 79N ice stream up flow from the site during the LGM (cf. Rea et al., 1998; Roberts et al., 2013; Sugden & Watts, 1977). Indeed, erratics from summit areas on Store Koldeway and Pusterdal (south of our study area) also show emplacement by ice across high elevation plateau terrain during the last glacial cycle (Skov et al., 2020). Furthermore, there is clear evidence of an elevationally-controlled transition to enhanced warm-based subglacial erosion below 460 m a.s.l. in the landscape around Dove Bugt. This finding accords with our own interpretation reported earlier highlighting enhanced subglacial erosion below 600 m a.s.l. and the development of scoured and abraded bedrock surfaces.

In general, there is limited evidence for moraines formed by local ice masses at high elevation. Only where local ice caps expanded and transitioned to polythermal outlet glaciers are moraines found at low elevations in the landscape. Hence, there is definitive evidence to support local ice cap fluctuation and expansion, which infers localized areas of blockfields have remained intact and undisturbed despite being overrun during the Holocene.

5.2 | Deglaciation and ice stream thinning

An assemblage of distinctive glacial landforms indicates the maximum thickness of the 79N ice stream during the LGM and subsequent thinning during deglaciation. From highest to lowest elevation, these features are streamlined bedrock terrain, lateral moraines, 'hummocky' moraine and perched deltas. This landform assemblage is found in various locations in the study area, most prominently as vertical staircases on the slopes and marginal valleys on the northern side of the 79N fjord.

5.2.1 | Streamlined bedrock terrain

Below the zone of allochthonous blockfields between 900 and 600 m a.s.l. striae and plucked bedrock surfaces (Figures 2 and 7a) confirm a thermal transition to warm-based ice flowing eastwards along the fjord. Areas of scoured bedrock are covered by patchy glacial sediment and a mixed assemblage of erratics which indicate ice flow sourced from the west (Pedersen et al., 2013). Sculpting and abrasion to form crude bedrock bedforms and roches moutonnées are typical of hard-bed processes dominated by basal sliding and commonly associated with areas of areal scour and ice streaming beneath outlet glaciers/isbræ from the Greenland Ice Sheet (e.g., Lane et al., 2015b; Roberts & Long, 2005; Skov et al., 2020). Less frequently reported in terrestrial settings in Greenland is evidence for subglacial sediment deformation (Lea et al., 2014; Pearce et al., 2018). Areas of streamlined drift and flutes adjacent to the northern 79N margin demonstrate ice was not only warm-based but operating over a deforming bed in places. Such conditions are common in submarginal locations associated with ice streams, with deforming bed tills playing a pivotal role in controlling ice stream dynamics and marginal stability (Ó Cofaigh et al., 2002; Ó Cofaigh et al., 2007; Roberson et al., 2011).

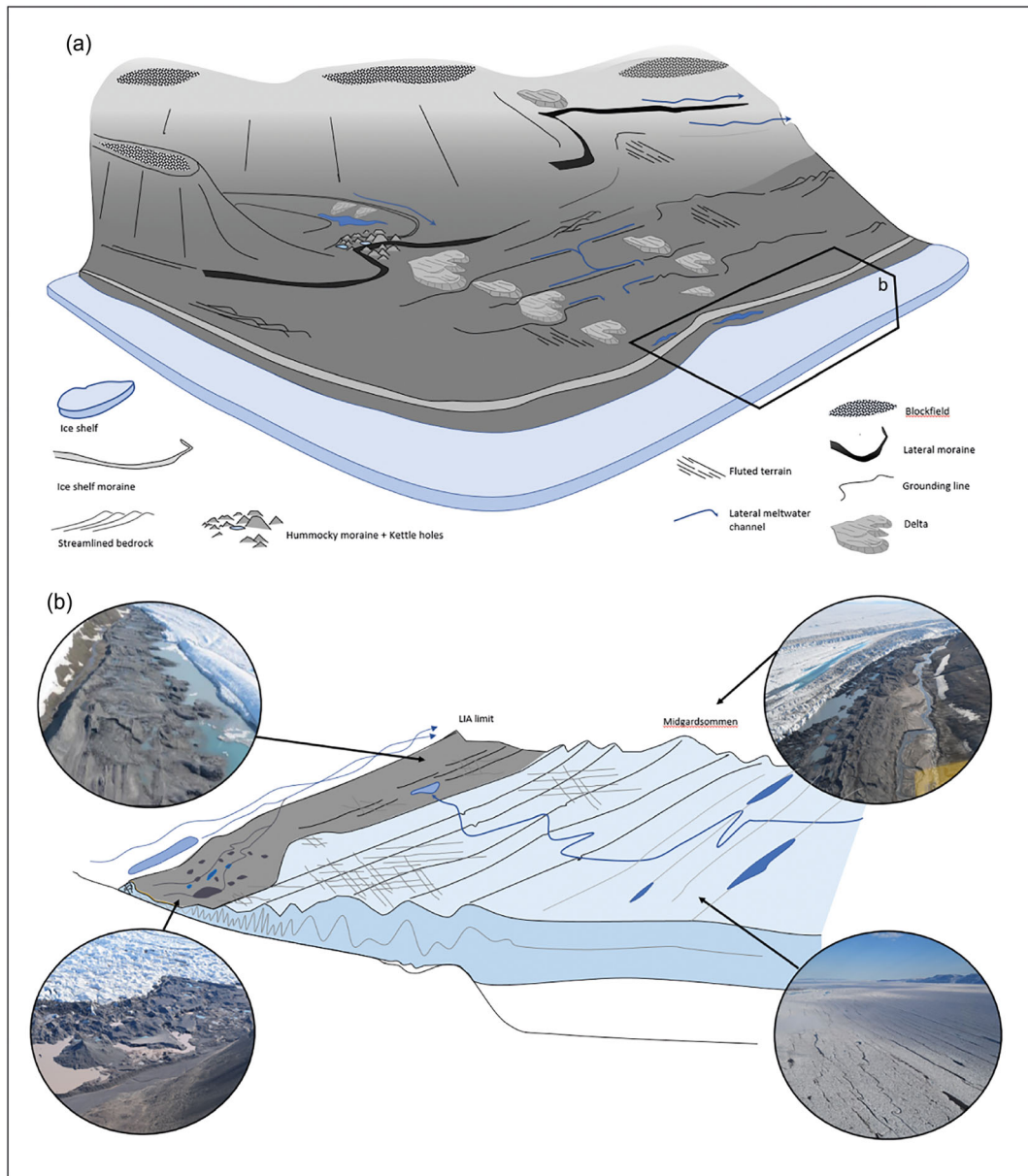


FIGURE 13 Conceptual diagrams of (a) ice stream to ice shelf deglacial transition marked along fjord walls by lateral moraines, streamlined grounding lines and delta staircases; and (b) the LIA/contemporary ice shelf margin characterized by ice shelf compressional ridges, push and controlled moraines; kames terraces; kame and kettle dead-ice terrain; ice marginal glaciofluvial corridors, and supraglacial drainage [Color figure can be viewed at wileyonlinelibrary.com]

5.2.2 | Lateral moraines

Distinctive arcuate moraine ridges on the northern side of the 79N fjord mark the limits of a thicker NEGIS which flowed north and eastwards across the high elevation landscape (Figure 11). Allochthonous blockfields occur above the moraines, highlighting the likely transition from cold- to warm-based ice. The highest elevation ridges at ~600 m a.s.l. record a minimum ice thickness of 1500 m within the trough. Many of these moraines skirt valley edges and topographic depressions, suggesting partially constrained ice. This juxtaposition of cold- and warm-based ice along a palaeo-ice stream margin has been noted elsewhere in Greenland (Roberts et al., 2013; Skov et al., 2020). For example, the Uummannaq ice stream produced similar high-elevation lateral moraines demonstrating that ice overtopped steep confining fjord walls and locally pushed onto high elevation plateau areas above ~750–800 m a.s.l. (Lane et al., 2014; Roberts et al., 2013). As the 79N ice stream thinned, it gradually withdrew

from the higher elevation landscape, depositing sequences of nested lateral moraine ridges north of 79N (Figure 11) and on Lambert Land (Figure 12), demonstrating periodic ice stream stabilization during overall deglaciation. This is similar to other ice stream marginal settings where thinning produces staircases of nested lateral moraines in fjord settings (Davies et al., 2017).

Zones of distinctive ‘hummocky’ moraine occur in places below arcuate moraine ridges, most notably at ~350–410 m a.s.l. in eastern Isakdalen (Figures 4 and 11). We attribute these features to ice contact/marginal deposition during ice stagnation. The steep proximal sides of the conical hummocks, partially sorted sediment and kettle holes are indicative of glaciofluvial fans or kames deposited in coalescent ice marginal settings where meltwater is routed between ice masses and where the subsequent secondary deposition of fluvio-glacial sediment begins to partially bury the ice margin. In Isakdalen, the topographic position of the hummocks demonstrate that they formed in a zone of coalescence between two retreating ice masses, with ice receding both to the

northwest into Isakdalen and southwards towards 79N (see centre of Figure 11d–f). Such suture zones provided conduits for the routing of meltwater, but also ice marginal environments within which water became ponded. The flat-topped surfaces of a number of hummocks further suggests ponding and ice-walled conditions in these coalescent zones (cf. Evans et al., 2017).

5.2.3 | Deltas

Large glacio-lacustrine deltas are particularly prominent at ~300–50 m a.s.l. in Isakdalen, and the valley to the north (Figures 4 and 11), with smaller equivalents found at ~60 m a.s.l. on Hovgaard Øer (Figures 5 and 12). These all exist above the marine limit, as reported by Bennike and Weidick (2001). We infer delta staircases record meltwater ponding at progressively lower elevations as the ice stream thinned during deglaciation (Figure 11d–f). The presence of ice dammed lakes indicates significant meltwater production and a quasi-stable terrestrial ice margin. Additionally, the evidence of a fluted, deforming bed associated with these ice margins supports the presence of warm-based active ice along the ice stream margin during deglaciation. Hence, delta staircases appear to record gradual lowering of the ice stream surface and emergence of the fjord walls during deglaciation.

5.2.4 | Ice stream landsystem summary

This landform assemblage (summarized in Figure 13a) resembles systems reported in northern Canada and Greenland where former grounded ice margins occurred above the local marine limit (England et al., 1978; Larsen et al., 2010; Möller et al., 2010). The perched deltas along the 79N fjord are particularly important geomorphological constraints on ice stream thinning and concomitant retreat of the grounding line from the outer coast to the inner fjord. Deglaciation of 79N from the outer coast to the inner fjord is presently constrained to 10.2–7.9 ka (Bennike & Weidick, 2001; Larsen et al., 2018) but these age constraints are from low elevation sites and do not capture evidence for antecedent thinning which may have conditioned a rapid grounding line retreat and ice shelf disintegration. The delta sequences record the emergence of the coastal mountains and fjord prior to 10.2 ka. The association of chains of ‘hummocky’ moraine composed of sorted sediment with arcuate moraines and deltas suggest the formation of kames and deltas as marginal meltwater began to flow and pond along the ice margin. Increased meltwater production implicates atmospheric warming as at least a partial driver of the deglaciation.

The delta staircases can be traced down to ~50 m a.s.l. in Isakdalen and ~65 m a.s.l. on Hovgaard Øer just above the local marine limit (Bennike & Weidick, 2001), tracking the thinning of a grounded ice margin until full deglaciation, after which sea-level began to fall (Bennike & Weidick, 2001). There is little evidence for a transition to an ice shelf from the mid- to inner-fjord during deglaciation, suggesting that the 79N ice stream may have remained grounded but was not fronted by an accompanying ice shelf as it passed through mid- to inner-fjord (Bennike & Weidick, 2001; Smith et al., 2022).

5.3 | Ice stream–ice shelf transition

5.3.1 | An Early Holocene ice shelf retreat signal in Nioghalvesfjerdjorden?

There is a clear geomorphological distinction between the terrestrial landforms generated during deglaciation by the grounded ice stream margin and landforms produced during a subsequent ice shelf (floating ice) expansion in the late Holocene (Bennike & Weidick, 2001; Smith et al., 2022). The regional marine limit ranges from c. 70–65 m a.s.l. in the east to 40–35 m a.s.l. in the west adjacent to Blåsø (Bennike & Weidick, 2001). The assemblage of lateral moraines, ‘hummocky’ moraine and staircases of perched deltas are found above this and records the thinning of the grounded ice stream margin (Figures 4, 6, and 7).

On Hovgaard Øer an upper ice shelf limit is marked by a moraine composed of grey glacial sediment (Figure 10). This hypothesized ice shelf limit is coincident with the marine limit at c. 65 m a.s.l. *Portlandia arctica* molluscs from the ice shelf moraine sediment have been dated to 9.8–9.5 cal. ka (Bennike & Weidick, 2001), confirming that this represents a deglacial phase ice shelf margin. Several key landforms including kettle holes, linear moraine ridges, ice marginal channels and kame terraces, and small ice marginal lakes mirror the geomorphological signal of the post-LIA ice shelf landsystem identified later. This ice shelf limit has been heavily degraded by periglacial activity, possibly confirming the antiquity of this particular area of Hovgaard Øer. Overprinting this Early Holocene ice shelf limit is a suite of landforms that relate to the later LIA ice shelf re-expansion.

The timing of ice retreat and thinning through 79N fjord can be bracketed by offshore and onshore deglacial ages. Deglaciation from the outer continental shelf was in progress by 15 ka (Stein et al., 1996), coincident with upstream ice sheet thinning along the fjord and emergence of the coastal mountains. Ice stream thinning would have been concomitant with grounding line retreat, which reached the outer coast and fjord mouth by c. 11.5–8.9 ka (Larsen et al., 2018). Ice subsequently began retreating through 79N fjord c. 10.2–7.9 ka (Larsen et al., 2018). Despite the localized evidence for an ice shelf on Hovgaard Øer at the opening of the Holocene, there is no confirmatory evidence of such an ice shelf in mid- or inner-fjord locations. The implication may be rapid grounding line retreat under tide-water conditions through Nioghalvesfjerdjorden, no substantive ice shelf. This hypothesis accords with Syring et al. (2020) who reported ice shelf disintegration prior to grounding line retreat inboard of the pinning point at the mouth of Nioghalvesfjerdjorden at c. 10.0–9.0 ka. It is further corroborated by evidence of open marine conditions in Blåsø by 8.5 ka (Bennike & Weidick, 2001; Larsen et al., 2018; Smith et al., 2022). The rapid breakup of an ice shelf during deglaciation has been reported in other High Arctic locations, with England et al. (2022) recording the catastrophic collapse of the Viscount Melville Sound ice shelf along the north-western Laurentide Ice Sheet, with ice shelf advance collapse occurring in 150 years.

5.3.2 | Neoglacial ice shelf regrowth

Along the northern margins of 79N the ice shelf landsystem has several distinct elements. Firstly, large, sharp-crested linear moraine

ridges are often composed of bulldozed and folded sediments suggesting many are ice shelf push moraines. Inboard of the outer linear moraine ridges are a series of smaller, ice flow parallel linear ridges (Figure 9). They are interpreted to represent compression, folding and foliation development along the margin of the ice shelf. They may originate from lateral compression of the ice stream proximal to the grounding line as it transitioned to a floating ice shelf or alternatively, they may be a product of localized lateral compression of the ice shelf margin. Folding related to either process may bring subglacial debris to the ice surface (Figure 13) and these may be a form of 'controlled' moraine (Evans, 2009; Hambrey et al., 2015). A further structural influence exerted by the ice shelf margin is manifest in the short, sinuous, and crenulated ridges that sit inboard of the ice shelf moraines. These are interpreted as remnants of crevasse infills (Evans et al., 2016) formed through the interaction of ice marginal or supraglacial streams with the ice shelf margin.

Given the position of the outermost, large linear moraine ridges, close to the current ice shelf margin (see Figure 9b), they are taken to mark the limit of 79N ice shelf during the LIA. Bennike and Weidick (2001) sampled reworked marine shells within these ridges which dated to the early Neoglacial, marking ice shelf re-expansion during the Mid- to Late-Holocene. This is supported by evidence from sediment cores in Blåssø which record ice shelf regrowth after 4.4 cal ka BP reaching its present thickness by 4.0 cal ka BP.

Depending on the ice shelf margin geometry and marginal fjord bathymetry, marginal lakes may be fully marine, epishelf, or transitional and are commonly associated with ice shelves in the Arctic (England et al., 1978, 2009; Hodgson & Vincent, 1984; Larsen et al., 2010; Möller et al., 2010) and Antarctic (Hambrey et al., 2015). We found no evidence of large-scale deltas forming in these lakes compared to the ice stream marginal landsystem outlined earlier – likely due to shallower water depths (fans are evident) and much smaller catchments with concomitant reduction in water and sediment supply. The lakes act as local sedimentary depo-centres and together with the fluvio-glacial corridors that form kame terraces lead to the development of a confined linear ice marginal landsystem similar to those reported from other ice shelf marginal settings in the Canadian High Arctic (England et al., 2009; Hodgson & Vincent, 1984). Importantly once the outer linear moraine ridges are breached, the glaciofluvial transport of sediment leads to the partial burial of the ice shelf margin and the potential for longer-term development of distinctive dead ice topography.

The ice shelf geomorphological signal that occurs below the marine limit records the advance of an ice shelf in the Late Holocene, likely starting in the Older Neoglacial and culminating in the LIA (Briner et al., 2016). Minimum ice extent in the early Holocene remains unknown. Larsen et al. (2018) speculated that the NEGIS grounding line was 20–70 km up-ice of the present-day grounding line between 7.8 and 1.2 ka, but Smith et al. (2022) record the ice shelf reforming at Blåssø by c. 4.4 cal ka BP. This is supported by earlier estimates of ice shelf re-growth as indicated by driftwood and whale bone from c. 5.4 cal ka BP (Bennike & Weidick, 2001).

Following the LIA, ice shelves fronting NEGIS have thinned, retreated and disintegrated. Over the last two decades the ZI ice shelf disintegrated after 2010 and the 79N ice shelf has thinned by 30% between 1999 to 2014 (Mayer et al., 2018). The rapid thinning of the 79N ice shelf has resulted in the ice shelf marginal landform signal

reported here (see Figures 9 and 13b). Its preservation potential is likely to be poor and ultimately dependent on the thickness of the ice shelf margin, structural glaciological controls, fjord wall geometry, the rate of buried dead-ice decay, relative sea-level fluctuation and reworking by secondary processes. Notably, geomorphological evidence of ice shelf thinning during deglaciation is sparse, because deglacial dates suggest the ice shelf collapsed leading to rapid grounding line retreat through the mid- to inner-79N fjord (Smith et al., 2022). In its present guise the rapidly evolving margin of the 79N ice shelf typifies the geomorphological signal of an ice shelf marginal landsystem in a rapidly warming climate where the rate of ice shelf thinning, rather than rapid grounding line retreat, is the key control on its morphostratigraphic signal, though this may rapidly change if the ice shelf starts to collapse.

6 | CONCLUSIONS

Our study shows that the geomorphological imprint of 79N records a lateral transition from a grounded ice stream to a floating ice shelf during deglaciation. Above 900 m a.s.l., terrain is covered by local ice caps or autochthonous blockfields. From 900 to 600 m a.s.l., autochthonous blockfields transition to allochthonous blockfields with local and far-travelled erratics, recording the lateral transition from cold- to warm-based and faster flowing ice within the fjord. Below 600 m a.s.l., lateral and 'hummocky' moraines, ice-contact deltas, and abraded bedrock provide evidence for a warm-based, grounded ice stream with a thinning margin. Landform evidence in the outer fjord at Hovgaard Øer records the presence of an ice shelf moraine, deposited during deglaciation. This geomorphological signal is absent along the rest of the fjord, suggesting ice shelf breakup prior to – or during – the onset of ice stream retreat through the fjord.

The 79N ice shelf expanded during the Neoglacial, reaching a maximum at the LIA, and subsequently thinned during the latter part of the 20th century with acceleration of the thinning during the 21st century. This has resulted in a suite of ice shelf moraines formed through marginal bulldozing with secondary controlled-moraine development, ice marginal epishelf and freshwater lakes, kame terraces and ice stagnation topography produced through ice marginal fluvio-glacial corridor development and sediment burial. Collectively, these record the geomorphological signal of a rapidly thinning ice shelf in a warming climate.

AUTHOR CONTRIBUTIONS

TPL, CMD, and DHR conceptualised the idea of the manuscript. DHR, BRR, MJB, SSRJ, JAS, and COC acquired funding for the project. TPL, CMD, MJB, JAS, SSRJ and DHR completed fieldwork. TPL, CMD, BRR, and DHR completed initial data analysis and wrote the initial draft. All authors assisted with editing the manuscript.

ACKNOWLEDGEMENTS

This work was funded through the Natural Environment Research Council Standard Grant NE/N011228/1. We thank the Alfred Wegener Institute and particularly Angelika Humbert and Hicham Rafiq for their logistic support through the iGRIFF project. Further support was provided from Station Nord (Jorgen Skafte), Nordland Air, Air Greenland, and the Joint Arctic Command. Naalakkersuisut, Government of Greenland, provided Scientific

Survey (VU-00121) and Export (046/2017) licences for this work. We thank Chris Orton for help with production of figures. Finally, we would like to thank our Field Ranger Isak (after which Isakdalen is informally named) and dog Ooni for keeping us safe in the field. We thank Rob Storrar and an anonymous reviewer for their comments which helped improve the manuscript.

DATA AVAILABILITY STATEMENT

Shapefile data will be stored on the UK Polar Data Centre; <https://www.bas.ac.uk/data/uk-pdc/>

ORCID

Timothy P. Lane  <https://orcid.org/0000-0002-7116-9976>

David H. Roberts  <https://orcid.org/0000-0002-5976-8423>

REFERENCES

- Andreassen, K., Winsborrow, M.C., Bjarnadóttir, L.R. & Rùther, D.C. (2014) Ice stream retreat dynamics inferred from an assemblage of landforms in the northern Barents Sea. *Quaternary Science Reviews*, 92, 246–257. Available from: <https://doi.org/10.1016/j.quascirev.2013.09.015>
- Antoniades, D., Francus, P., Pienitz, R., St-Onge, G. & Vincent, W.F. (2011) Holocene dynamics of the Arctic's largest ice shelf. *Proceedings of the National Academy of Sciences*, 108(47), 18899–18904. Available from: <https://doi.org/10.1073/pnas.1106378108>
- Arndt, J.E., Jokat, W. & Dorschel, B. (2017) The last glaciation and deglaciation of the Northeast Greenland continental shelf revealed by hydro-acoustic data. *Quaternary Science Reviews*, 160, 45–56. Available from: <https://doi.org/10.1016/j.quascirev.2017.01.018>
- Arndt, J.E., Jokat, W., Dorschel, B., Myklebust, R., Dowdeswell, J.A. & Evans, J. (2015) A new bathymetry of the Northeast Greenland continental shelf: Constraints on glacial and other processes. *Geochemistry, Geophysics, Geosystems*, 16(10), 3733–3753. Available from: <https://doi.org/10.1002/2015GC005931>
- Ballantyne, C.K. (2018) *Periglacial geomorphology*. Hoboken, NJ, USA: John Wiley & Sons.
- Batchelor, C. & Dowdeswell, J. (2015) Ice-sheet grounding-zone wedges (GZWs) on high-latitude continental margins. *Marine Geology*, 363, 65–92. Available from: <https://doi.org/10.1016/j.margeo.2015.02.001>
- Batchelor, C. & Dowdeswell, J. (2016) Lateral shear-moraines and lateral marginal-moraines of palaeo-ice streams. *Quaternary Science Reviews*, 151, 1–26. Available from: <https://doi.org/10.1016/j.quascirev.2016.08.020>
- Beel, C., Lifton, N., Briner, J. & Goehring, B. (2016) Quaternary evolution and ice sheet history of contrasting landscapes in Uummannaq and Sukkertoppen, western Greenland. *Quaternary Science Reviews*, 149, 248–258. Available from: <https://doi.org/10.1016/j.quascirev.2016.05.033>
- Benn, D. & Evans, D.J. (2014) *Glaciers and glaciation*. London: Routledge [10.4324/9780203785010](https://doi.org/10.4324/9780203785010).
- Benn, D.I. (1992) The genesis and significance of 'hummocky moraine': Evidence from the Isle of Skye, Scotland. *Quaternary Science Reviews*, 11(7–8), 781–799. Available from: [https://doi.org/10.1016/0277-3791\(92\)90083-K](https://doi.org/10.1016/0277-3791(92)90083-K)
- Bennike, O. & Weidick, A. (2001) Late Quaternary history around Nioghalvfjærdsfjorden and Jøkelbugten, north-East Greenland. *Boreas*, 30(3), 205–227. Available from: <https://doi.org/10.1080/030094801750424139>
- Bentley, M., Hodgson, D., Sugden, D., Roberts, S., Smith, J., Leng, M., et al. (2005) Early Holocene retreat of the George VI ice shelf, Antarctic peninsula. *Geology*, 33(3), 173–176. Available from: <https://doi.org/10.1130/G21203.1>
- Bentley, M.J., Smith, J.A., Jamieson, S.S., Lindeman, M., Rea, B.R., Humbert, A., et al. (2022) Direct measurement of warm Atlantic intermediate water close to the grounding line of Nioghalvfjærdsfjorden (79N) glacier, north-East Greenland. *The Cryosphere Discussions*, 1–25. Available from: <https://doi.org/10.5194/tc-2022-206>
- Briner, J.P., Lifton, N.A., Miller, G.H., Refsnider, K., Anderson, R. & Finkel, R. (2014) Using in situ cosmogenic ¹⁰Be, ¹⁴C, and ²⁶Al to decipher the history of polythermal ice sheets on Baffin Island, Arctic Canada. *Quaternary Geochronology*, 19, 4–13. Available from: <https://doi.org/10.1016/j.quageo.2012.11.005>
- Briner, J.P., McKay, N.P., Axford, Y., Bennike, O., Bradley, R.S., De Vernal, A., et al. (2016) Holocene climate change in Arctic Canada and Greenland. *Quaternary Science Reviews*, 147, 340–364. Available from: <https://doi.org/10.1016/j.quascirev.2016.02.010>
- Chandler, B.M., Lovell, H., Boston, C.M., Lukas, S., Barr, I.D., Benediktsson, Í.Ö., et al. (2018) Glacial geomorphological mapping: A review of approaches and frameworks for best practice. *Earth-Science Reviews*, 185, 806–846. Available from: <https://doi.org/10.1016/j.earscirev.2018.07.015>
- Choi, Y., Morlighem, M., Rignot, E., Mouginot, J. & Wood, M. (2017) Modeling the response of Nioghalvfjærdsfjorden and Zachariae Isstrøm glaciers, Greenland, to ocean forcing over the next century. *Geophysical Research Letters*, 44(21), 11,071–11,079. Available from: <https://doi.org/10.1002/2017GL075174>
- Couette, P.-O., Lajeunesse, P., Ghienne, J.-F., Dorschel, B., Gebhardt, C., Hebbeln, D., et al. (2022) Evidence for an extensive ice shelf in northern Baffin Bay during the last glacial maximum. *Communications Earth & Environment*, 3, 1–12.
- Dahl, R. (1966) Block fields, weathering pits and tor-like forms in the Narvik Mountains, Nordland, Norway. *Geografiska Annaler. Series A, Physical Geography*, 48(2), 55–85. Available from: <https://doi.org/10.1080/04353676.1966.11879730>
- Davies, B.J., Hambrey, M.J., Glasser, N.F., Holt, T., Rodés, A., Smellie, J.L., et al. (2017) Ice-dammed lateral lake and epishelf lake insights into Holocene dynamics of Marguerite trough ice stream and George VI ice shelf, Alexander island, Antarctic peninsula. *Quaternary Science Reviews*, 177, 189–219. Available from: <https://doi.org/10.1016/j.quascirev.2017.10.016>
- Davies, J., Mathiasen, A.M., Kristiansen, K., Hansen, K.E., Wacker, L., Alstrup, A.K.O., et al. (2022) Linkages between ocean circulation and the Northeast Greenland ice stream in the Early Holocene. *Quaternary Science Reviews*, 286, 107530. Available from: <https://doi.org/10.1016/j.quascirev.2022.107530>
- Dowdeswell, J., Batchelor, C., Montelli, A., Ottesen, D., Christie, F., Dowdeswell, E., et al. (2020) Delicate seafloor landforms reveal past Antarctic grounding-line retreat of kilometers per year. *Science*, 368(6494), 1020–1024. Available from: <https://doi.org/10.1126/science.aaz3059>
- Dowdeswell, J. & Fugelli, E. (2012) The seismic architecture and geometry of grounding-zone wedges formed at the marine margins of past ice sheets. *Bulletin*, 124, 1750–1761.
- Dowdeswell, J.A. & Jeffries, M.O. (2017) *Arctic ice shelves: An introduction*. In: Copland, L. & Mueller, D. (Eds.) *Arctic ice shelves and ice islands* (pp. 3–21). Dordrecht: Springer Netherlands.
- England, J., Bradley, R.S. & Miller, G. (1978) Former ice shelves in the Canadian high Arctic. *Journal of Glaciology*, 20(83), 393–404. Available from: <https://doi.org/10.1017/S0022143000013927>
- England, J., Coulthard, R., Furze, M. & Dow, C. (2022) Catastrophic ice shelf collapse along the NW Laurentide ice sheet highlights the vulnerability of marine-based ice margins. *Quaternary Science Reviews*, 286, 107524. Available from: <https://doi.org/10.1016/j.quascirev.2022.107524>
- England, J.H., Furze, M.F. & Doupe, J.P. (2009) Revision of the NW Laurentide ice sheet: Implications for paleoclimate, the northeast extremity of Beringia, and Arctic Ocean sedimentation. *Quaternary Science Reviews*, 28(17–18), 1573–1596. Available from: <https://doi.org/10.1016/j.quascirev.2009.04.006>
- Evans, D.J. (2009) Controlled moraines: Origins, characteristics and palaeogeological implications. *Quaternary Science Reviews*, 28(3–4), 183–208. Available from: <https://doi.org/10.1016/j.quascirev.2008.10.024>
- Evans, D.J., Hughes, A.L., Hansom, J.D. & Roberts, D.H. (2017) Scottish landform examples 43: Glacifluvial landforms of Strathallan,

- Perthshire. *Scottish Geographical Journal*, 133(1), 42–53. Available from: <https://doi.org/10.1080/14702541.2016.1254276>
- Evans, D.J., Rea, B.R., Hansom, J.D. & Whalley, W.B. (2002) Geomorphology and style of plateau icefield deglaciation in fjord terrains: The example of Troms-Finnmark, North Norway. *Journal of Quaternary Science: Published for the Quaternary Research Association*, 17(3), 221–239. Available from: <https://doi.org/10.1002/jqs.675>
- Evans, D.J., Storrar, R.D. & Rea, B.R. (2016) Crevasse-squeeze ridge corridors: Diagnostic features of late-stage palaeo-ice stream activity. *Geomorphology*, 258, 40–50. Available from: <https://doi.org/10.1016/j.geomorph.2016.01.017>
- Evans, J., Ó Cofaigh, C., Dowdeswell, J.A. & Wadhams, P. (2009) Marine geophysical evidence for former expansion and flow of the Greenland ice sheet across the north-East Greenland continental shelf. *Journal of Quaternary Science: Published for the Quaternary Research Association*, 24(3), 279–293. Available from: <https://doi.org/10.1002/jqs.1231>
- Fahnestock, M., Bindschadler, R., Kwok, R. & Jezek, K. (1993) Greenland ice sheet surface properties and ice dynamics from ERS-1 SAR imagery. *Science*, 262(5139), 1530–1534. Available from: <https://doi.org/10.1126/science.262.5139.1530>
- Franke, S., Jansen, D., Binder, T., Dörr, N., Helm, V., Paden, J., et al. (2020) Bed topography and subglacial landforms in the onset region of the Northeast Greenland ice stream. *Annals of Glaciology*, 61(81), 143–153. Available from: <https://doi.org/10.1017/aog.2020.12>
- Freire, F., Gyllencreutz, R., Greenwood, S.L., Mayer, L., Egilsson, A., Thorsteinsson, T., et al. (2015) High resolution mapping of offshore and onshore glaciogenic features in metamorphic bedrock terrain, Melville Bay, northwestern Greenland. *Geomorphology*, 250, 29–40. Available from: <https://doi.org/10.1016/j.geomorph.2015.08.011>
- Furze, M.F., Pierikowski, A.J., McNeely, M.A., Bennett, R. & Cage, A.G. (2018) Deglaciation and ice shelf development at the northeast margin of the Laurentide ice sheet during the younger Dryas chronozone. *Boreas*, 47(1), 271–296. Available from: <https://doi.org/10.1111/bor.12265>
- Gardner, A.S., Fahnestock, M.A. & Scambos, T.A. (2019) ITS_LIVE regional glacier and ice sheet surface velocities. Data archived at National Snow and Ice Data Center, 10.
- Gardner, A.S., Moholdt, G., Scambos, T., Fahnestock, M., Ligtenberg, S., Van Den Broeke, M., et al. (2018) Increased West Antarctic and unchanged East Antarctic ice discharge over the last 7 years. *The Cryosphere*, 12(2), 521–547. Available from: <https://doi.org/10.5194/tc-12-521-2018>
- Gibson, J.A. & Andersen, D.T. (2002) Physical structure of epishelf lakes of the southern Bunge Hills, East Antarctica. *Antarctic Science*, 14(3), 253–261. Available from: <https://doi.org/10.1017/S095410200200010X>
- Glasser, N., Goodsell, B., Copland, L. & Lawson, W. (2006) Debris characteristics and ice-shelf dynamics in the ablation region of the McMurdo ice shelf, Antarctica. *Journal of Glaciology*, 52(177), 223–234. Available from: <https://doi.org/10.3189/172756506781828692>
- Goldberg, D., Holland, D. & Schoof, C. (2009) Grounding line movement and ice shelf buttressing in marine ice sheets. *Journal of Geophysical Research - Earth Surface*, 114, F04026.
- Graham, A.G., Larter, R.D., Gohl, K., Hillenbrand, C.-D., Smith, J.A. & Kuhn, G. (2009) Bedform signature of a West Antarctic palaeo-ice stream reveals a multi-temporal record of flow and substrate control. *Quaternary Science Reviews*, 28(25–26), 2774–2793. Available from: <https://doi.org/10.1016/j.quascirev.2009.07.003>
- Gudmundsson, G. (2013) Ice-shelf buttressing and the stability of marine ice sheets. *The Cryosphere*, 7(2), 647–655. Available from: <https://doi.org/10.5194/tc-7-647-2013>
- Hambrey, M.J., Davies, B.J., Glasser, N.F., Holt, T.O., Smellie, J.L. & Carrivick, J.L. (2015) Structure and sedimentology of George VI ice shelf, Antarctic peninsula: Implications for ice-sheet dynamics and landform development. *Journal of the Geological Society*, 172(5), 599–613. Available from: <https://doi.org/10.1144/jgs2014-134>
- Hodgson, D.A. & Vincent, J.-S. (1984) A 10,000 yr BP extensive ice shelf over viscount Melville sound, Arctic Canada. *Quaternary Research*, 22(1), 18–30. Available from: [https://doi.org/10.1016/0033-5894\(84\)90003-6](https://doi.org/10.1016/0033-5894(84)90003-6)
- Hogg, A.E., Shepherd, A., Gourmelen, N. & Engdahl, M. (2016) Grounding line migration from 1992 to 2011 on Petermann glacier, north-West Greenland. *Journal of Glaciology*, 62(236), 1104–1114. Available from: <https://doi.org/10.1017/jog.2016.83>
- Jakobsson, M., Mayer, L.A., Bringenspar, C., Castro, C.F., Mohammad, R., Johnson, P., et al. (2020) The international bathymetric chart of the Arctic Ocean version 4.0. *Scientific Data*, 7(1), 176.
- Jezek, K., Wu, X., Gogineni, P., Rodríguez, E., Freeman, A., Rodríguez-Morales, F., et al. (2011) Radar images of the bed of the Greenland ice sheet. *Geophysical Research Letters*, 38(1), n/a. Available from: <https://doi.org/10.1029/2010GL045519>
- Johnson, J.S., Bentley, M.J., Smith, J.A., Finkel, R., Rood, D., Gohl, K., et al. (2014) Rapid thinning of Pine Island glacier in the early Holocene. *Science*, 343(6174), 999–1001. Available from: <https://doi.org/10.1126/science.1247385>
- Joughin, I., Smith, B.E., Howat, I.M., Scambos, T. & Moon, T. (2010) Greenland flow variability from ice-sheet-wide velocity mapping. *Journal of Glaciology*, 56(197), 415–430. Available from: <https://doi.org/10.3189/002214310792447734>
- Kaufman, D.S., Ager, T.A., Anderson, N.J., Anderson, P.M., Andrews, J.T., Bartlein, P.J., et al. (2004) Holocene thermal maximum in the western Arctic (0–180 W). *Quaternary Science Reviews*, 23(5–6), 529–560. Available from: <https://doi.org/10.1016/j.quascirev.2003.09.007>
- Kessler, M.A., Anderson, R.S. & Briner, J.P. (2008) Fjord insertion into continental margins driven by topographic steering of ice. *Nature Geoscience*, 1(6), 365–369. Available from: <https://doi.org/10.1038/ngeo201>
- Khan, S.A., Kjær, K.H., Bevis, M., Bamber, J.L., Wahr, J., Kjeldsen, K.K., et al. (2014) Sustained mass loss of the Northeast Greenland ice sheet triggered by regional warming. *Nature Climate Change*, 4(4), 292–299. Available from: <https://doi.org/10.1038/nclimate2161>
- Kleman, J., Hätteland, C., Borgström, I. & Stroeven, A. (1997) Fennoscandian palaeoglaciology reconstructed using a glacial geological inversion model. *Journal of Glaciology*, 43(144), 283–299. Available from: <https://doi.org/10.1017/S0022143000003233>
- Lane, T.P., Roberts, D.H., Ó Cofaigh, C., Rea, B.R. & Vieli, A. (2016) Glacial landscape evolution in the Uummannaq region, West Greenland. *Boreas*, 45(2), 220–234. Available from: <https://doi.org/10.1111/bor.12150>
- Lane, T.P., Roberts, D.H., Ó Cofaigh, C., Vieli, A. & Moreton, S.G. (2015a) The glacial history of the southern Svartenhuk Halvø, West Greenland. *Arktos*, 1, 1–28.
- Lane, T.P., Roberts, D.H., Rea, B.R., Cofaigh, C.Ó. & Vieli, A. (2015b) Controls on bedrock bedform development beneath the Uummannaq ice stream onset zone, West Greenland. *Geomorphology*, 231, 301–313. Available from: <https://doi.org/10.1016/j.geomorph.2014.12.019>
- Lane, T.P., Roberts, D.H., Rea, B.R., Cofaigh, C.Ó., Vieli, A. & Rodés, A. (2014) Controls upon the last glacial maximum deglaciation of the northern Uummannaq ice stream system, West Greenland. *Quaternary Science Reviews*, 92, 324–344. Available from: <https://doi.org/10.1016/j.quascirev.2013.09.013>
- Larsen, N.K., Kjær, K.H., Funder, S., Möller, P., Van Der Meer, J.J., Schomacker, A., et al. (2010) Late Quaternary glaciation history of northernmost Greenland—evidence of shelf-based ice. *Quaternary Science Reviews*, 29, 3399–3414.
- Larsen, N.K., Levy, L.B., Carlson, A.E., Buizert, C., Olsen, J., Strunk, A., et al. (2018) Instability of the Northeast Greenland ice stream over the last 45,000 years. *Nature Communications*, 9, 1–8.
- Lea, J.M., Mair, D.W., Nick, F.M., Rea, B.R., Weidick, A., Kjaer, K.H., et al. (2014) Terminus-driven retreat of a major Southwest Greenland tide-water glacier during the early 19th century: Insights from glacier reconstructions and numerical modelling. *Journal of Glaciology*, 60(2022), 333–344. Available from: <https://doi.org/10.3189/2014JoG13J163>
- Mackintosh, A.N., Verleyen, E., O'Brien, P.E., White, D.A., Jones, R.S., McKay, R., et al. (2014) Retreat history of the East Antarctic ice sheet since the last glacial maximum. *Quaternary Science Reviews*, 100, 10–30. Available from: <https://doi.org/10.1016/j.quascirev.2013.07.024>

- Mayer, C., Schaffer, J., Hattermann, T., Floricioiu, D., Krieger, L., Dodd, P. A., et al. (2018) Large ice loss variability at Nioghalvfjærdsfjorden glacier, Northeast-Greenland. *Nature Communications*, 9, 1–11.
- Möller, P., Larsen, N.K., Kjær, K.H., Funder, S., Schomacker, A., Linge, H., et al. (2010) Early to middle Holocene valley glaciations on northernmost Greenland. *Quaternary Science Reviews*, 29, 3379–3398.
- Moon, T., Fisher, M., Harden, L. & Stafford, T. (2021) QGreenland (v1.0.1) [software]. <https://qgreenland.org>
- Morlighem, M., Williams, C.N., Rignot, E., An, L., Arndt, J.E., Bamber, J.L., et al. (2017) BedMachine v3: Complete bed topography and ocean bathymetry mapping of Greenland from multibeam echo sounding combined with mass conservation. *Geophysical Research Letters*, 44(21), 11051–11061. Available from: <https://doi.org/10.1002/2017GL074954>
- Mouginot, J., Rignot, E., Scheuchl, B., Fenty, I., Khazendar, A., Morlighem, M., et al. (2015) Fast retreat of Zachariæ Isstrøm, Northeast Greenland. *Science*, 350(6266), 1357–1361. Available from: <https://doi.org/10.1126/science.aac7111>
- Newton, A., Knutz, P., Huuse, M., Gannon, P., Brocklehurst, S., Clausen, O., et al. (2017) Ice stream reorganization and glacial retreat on the Northwest Greenland shelf. *Geophysical Research Letters*, 44(15), 7826–7835. Available from: <https://doi.org/10.1002/2017GL073690>
- Nielsen, L.T., Aðalgeirsdóttir, G., Gkinis, V., Nuterman, R. & Hvidberg, C.S. (2018) The effect of a Holocene climatic optimum on the evolution of the Greenland ice sheet during the last 10 kyr. *Journal of Glaciology*, 64(245), 477–488. Available from: <https://doi.org/10.1017/jog.2018.40>
- Ó Cofaigh, C., Dowdeswell, J.A., Evans, J. & Larter, R.D. (2008) Geological constraints on Antarctic palaeo-ice-stream retreat. *Earth Surface Processes and Landforms: The Journal of the British Geomorphological Research Group*, 33(4), 513–525. Available from: <https://doi.org/10.1002/esp.1669>
- Ó Cofaigh, C., Dowdeswell, J.A., Jennings, A.E., Hogan, K.A., Kilfeather, A., Hiemstra, J.F., et al. (2013) An extensive and dynamic ice sheet on the West Greenland shelf during the last glacial cycle. *Geology*, 41(2), 219–222. Available from: <https://doi.org/10.1130/G33759.1>
- Ó Cofaigh, C., Evans, J., Dowdeswell, J.A. & Larter, R.D. (2007) Till characteristics, genesis and transport beneath Antarctic paleo-ice streams. *Journal of Geophysical Research - Earth Surface*, 112, F03006.
- Ó Cofaigh, C., Pudsey, C.J., Dowdeswell, J.A. & Morris, P. (2002) Evolution of subglacial bedforms along a paleo-ice stream, Antarctic peninsula continental shelf. *Geophysical Research Letters*, 29, 41–1–41-4.
- Pearce, D.M., Mair, D.W., Rea, B.R., Lea, J.M., Schofield, J.E., Kamenos, N., et al. (2018) The glacial geomorphology of upper Godthåbsfjord (Nuup Kangerlua) in Southwest Greenland. *Journal of Maps*, 14(2), 45–55. Available from: <https://doi.org/10.1080/17445647.2017.1422447>
- Pedersen, M., Weng, W.L., Keulen, N. & Kokfelt, T.F. (2013) A new seamless digital 1: 500 000 scale geological map of Greenland. *GEUS Bulletin*, 28, 65–68. Available from: <https://doi.org/10.34194/geusb.v28.4727>
- Rea, B.R., Whalley, W.B., Evens, D., Gordon, J.E. & McDougall, D.A. (1998) Plateau icefields: Geomorphology and dynamics. *Journal of Quaternary Science*, 13, 35–54.
- Rea, B.R., Whalley, W.B., Rainey, M.M. & Gordon, J.E. (1996) Blockfields, old or new? Evidence and implications from some plateaus in northern Norway. *Geomorphology*, 15(2), 109–121. Available from: [https://doi.org/10.1016/0169-555X\(95\)00118-0](https://doi.org/10.1016/0169-555X(95)00118-0)
- Reese, R., Gudmundsson, G.H., Levermann, A. & Winkelmann, R. (2018) The far reach of ice-shelf thinning in Antarctica. *Nature Climate Change*, 8(1), 53–57. Available from: <https://doi.org/10.1038/s41558-017-0020-x>
- Rignot, E., Jacobs, S., Mouginot, J. & Scheuchl, B. (2013) Ice-shelf melting around Antarctica. *Science*, 341(6143), 266–270. Available from: <https://doi.org/10.1126/science.1235798>
- Roberson, S., Hubbard, B., Coulson, H.R. & Boomer, I. (2011) Physical properties and formation of flutes at a polythermal valley glacier: Midre Lovénbreen, Svalbard. *Geografiska Annaler. Series A, Physical Geography*, 93(2), 71–88. Available from: <https://doi.org/10.1111/j.1468-0459.2011.00420.x>
- Roberts, D.H. & Long, A. (2005) Streamlined bedrock terrain and fast ice flow, Jakobshavns Isbrae, West Greenland: Implications for ice stream and ice sheet dynamics. *Boreas*, 34(1), 25–42. Available from: <https://doi.org/10.1080/03009480510012818>
- Roberts, D.H., Long, A.J., Davies, B.J., Simpson, M.J. & Schnabel, C. (2010) Ice stream influence on West Greenland ice sheet dynamics during the last glacial maximum. *Journal of Quaternary Science*, 25(6), 850–864. Available from: <https://doi.org/10.1002/jqs.1354>
- Roberts, D.H., Rea, B.R., Lane, T.P., Schnabel, C. & Rodés, A. (2013) New constraints on Greenland ice sheet dynamics during the last glacial cycle: Evidence from the Uumannaq ice stream system. *Journal of Geophysical Research - Earth Surface*, 118(2), 519–541. Available from: <https://doi.org/10.1002/jgrf.20032>
- Roberts, S., Hodgson, D., Bentley, M., Smith, J., Millar, I., Olive, V., et al. (2008) The Holocene history of George VI ice shelf, Antarctic peninsula from clast-provenance analysis of epishelf lake sediments. *Palaeogeography, Palaeoclimatology, Palaeoecology*, 259(2–3), 258–283. Available from: <https://doi.org/10.1016/j.palaeo.2007.10.010>
- Scambos, T.A., Bohlander, J., Shuman, C.A. & Skvarca, P. (2004) Glacier acceleration and thinning after ice shelf collapse in the Larsen B embayment, Antarctica. *Geophysical Research Letters*, 31(18), L18402. Available from: <https://doi.org/10.1029/2004GL020670>
- Schaffer, J., Kanzow, T., Von Appen, W.-J., Von Albedyll, L., Arndt, J.E. & Roberts, D.H. (2020) Bathymetry constrains ocean heat supply to Greenland's largest glacier tongue. *Nature Geoscience*, 13(3), 227–231. Available from: <https://doi.org/10.1038/s41561-019-0529-x>
- Skov, D.S., Andersen, J., Olsen, J., Jacobsen, B., Knudsen, M., Jansen, J., et al. (2020) Constraints from cosmogenic nuclides on the glaciation and erosion history of dove Bugt, Northeast Greenland. *GSA Bulletin*, 132(11–12), 2282–2294. Available from: <https://doi.org/10.1130/B35410.1>
- Smith, J.A., Andersen, T., Shortt, M., Gaffney, A., Truffer, M., Stanton, T.P., et al. (2017) Sub-ice-shelf sediments record history of twentieth-century retreat of Pine Island glacier. *Nature*, 541(7635), 77–80. Available from: <https://doi.org/10.1038/nature20136>
- Smith, J.A., Bentley, M.J., Hodgson, D.A., Roberts, S.J., Leng, M.J., Lloyd, J. M., et al. (2007) Oceanic and atmospheric forcing of early Holocene ice shelf retreat, George VI ice shelf, Antarctica peninsula. *Quaternary Science Reviews*, 26(3–4), 500–516. Available from: <https://doi.org/10.1016/j.quascirev.2006.05.006>
- Smith, J.A., Callard, L., Bentley, M.J., Jamieson, S.S., Sánchez-Montes, M.L., Lane, T.P., et al. (2022) Holocene history of 79° N ice shelf reconstructed from epishelf lake and uplifted glacial marine sediments. *The Cryosphere Discussions*, 1–38. Available from: <https://doi.org/10.5194/tc-2022-173>.
- Smith, J.A., Graham, A.G., Post, A.L., Hillenbrand, C.-D., Bart, P.J. & Powell, R.D. (2019) The marine geological imprint of Antarctic ice shelves. *Nature Communications*, 10, 1–16.
- Smith, J.A., Hodgson, D.A., Bentley, M.J., Verleyen, E., Leng, M.J. & Roberts, S.J. (2006) Limnology of two Antarctic epishelf lakes and their potential to record periods of ice shelf loss. *Journal of Paleolimnology*, 35(2), 373–394. Available from: <https://doi.org/10.1007/s10933-005-1333-8>
- Stein, R., Nam, S.-I., Grobe, H. & Hubberten, H. (1996) Late Quaternary glacial history and short-term ice-rafted debris fluctuations along the East Greenland continental margin. *Geological Society, London, Special Publications*, 111(1), 135–151. Available from: <https://doi.org/10.1144/GSL.SP.1996.111.01.09>
- Stokes, C.R. & Clark, C.D. (2003) The Dubawnt Lake palaeo-ice stream: Evidence for dynamic ice sheet behaviour on the Canadian shield and insights regarding the controls on ice-stream location and vigour. *Boreas*, 32(1), 263–279. Available from: <https://doi.org/10.1111/j.1502-3885.2003.tb01442.x>
- Strunk, A., Knudsen, M.F., Egholm, D.L., Jansen, J.D., Levy, L.B., Jacobsen, B.H., et al. (2017) One million years of glaciation and denudation history in West Greenland. *Nature Communications*, 8, 1–8.

- Sugden, D. (1974) Landscapes of glacial erosion in Greenland and their relationship to ice, topographic and bedrock conditions. *Institute of British Geographers Special Publication*, 7, 177–195.
- Sugden, D. & Clapperton, C. (1981) An ice-shelf moraine, George VI sound, Antarctica. *Annals of Glaciology*, 2, 135–141.
- Sugden, D.E. & Watts, S. (1977) Tors, felsenmeer, and glaciation in northern Cumberland peninsula, Baffin Island. *Canadian Journal of Earth Sciences*, 14(12), 2817–2823. Available from: <https://doi.org/10.1139/e77-248>
- Syring, N., Lloyd, J.M., Stein, R., Fahl, K., Roberts, D.H., Callard, L., et al. (2020) Holocene interactions between glacier retreat, sea ice formation, and Atlantic water advection at the inner Northeast Greenland continental shelf. *Paleoceanography and Paleoclimatology*, 35, e2020PA004019.
- Winkelmann, D., Jokat, W., Jensen, L. & Schenke, H.-W. (2010) Submarine end moraines on the continental shelf off NE Greenland – Implications for Lateglacial dynamics. *Quaternary Science Reviews*, 29(9–10), 1069–1077. Available from: <https://doi.org/10.1016/j.quascirev.2010.02.002>
- Xie, S., Dixon, T.H., Voytenko, D., Deng, F. & Holland, D.M. (2018) Grounding line migration through the calving season at Jakobshavn Isbræ, Greenland, observed with terrestrial radar interferometry. *The Cryosphere*, 12(4), 1387–1400. Available from: <https://doi.org/10.5194/tc-12-1387-2018>

How to cite this article: Lane, T.P., Darvill, C., Rea, B.R., Bentley, M.J., Smith, J.A., Jamieson, S.S.R. et al. (2023) The geomorphological record of an ice stream to ice shelf transition in Northeast Greenland. *Earth Surface Processes and Landforms*, 48(7), 1321–1341. Available from: <https://doi.org/10.1002/esp.5552>